Drug Design, Development and Therapy

Dovepress
Taylor & Francis Group

Open Access Full Text Article

ORIGINAL RESEARCH

7-Hydroxyethyl Chrysin Alleviates High Altitude Pulmonary Edema via Activation of the PI3K/AKT Signaling Pathway

Gege Wang[1,2], Ning Wang[2], Yu Xin[1,2], Huiping Ma[2], Linlin Jing[1]

[1]Department of Pharmacy, The First Affiliated Hospital of Xi'an Jiaotong University, Xi'an, Shaanxi, People's Republic of China; [2]Department of Pharmacy, The 940th Hospital of Joint Logistics Support Force of PLA, Lanzhou, Gansu, People's Republic of China

Correspondence: Linlin Jing, Department of Pharmacy, The First Affiliated Hospital of Xi'an Jiaotong University, No. 277 Yanta West Road, Yanta District, Xi'an, Shaanxi, 710061, People's Republic of China, Email jinglinlin@xjtufh.edu.cn; Huiping Ma, Department of pharmacy, The 940th Hospital of Joint Logistics Support force of PLA, No. 333 Binhe South Road, Qilihe District, Lanzhou, Gansu, 730050, People's Republic of China, Email huipingmacyk@163.com

Background: High-altitude pulmonary edema (HAPE) is a severe and potentially fatal complication without effective and safe measures. 7-hydroxyethyl chrysin (7-HEC) is a derivative of chrysin and exhibits excellent anti-hypoxia activities. The objective of this study was to investigate the protective effect and mechanism of 7-HEC against HAPE.

Methods: The HAPE rat model was established using a hypobaric hypoxic cabin. The lung water content (LWC) and pulmonary microvascular permeability were measured, and the pathological changes of lung tissue were assessed by HE staining. The arterial blood gas indexes and routine blood indexes were measured. The levels of oxidative stress, inflammatory, energy metabolism and endothelial function markers in lung tissue or serum were quantified by commercial kits. qRT-PCR and Western blotting were employed to analyze the expressions of inflammatory and permeability associated genes and proteins. Network pharmacology and molecular docking were performed to reveal the pivotal targets of 7-HEC against HAPE and underlying mechanisms.

Results: 7-HEC treatment reduced the LWC, attenuated pulmonary microvascular hyperpermeability, and improved lung tissue pathology in HAPE rats. Moreover, 7-HEC treatment normalized HAPE-induced changes in arterial blood gas and routine blood parameters. In addition, 7-HEC treatment significantly inhibited oxidative stress and inflammation, suppressed the energy metabolism dysfunction, and maintained the endothelial function. PI3K/AKT signaling pathway was identified as the core pathway for 7-HEC against HAPE by the results of network pharmacology analysis, molecular docking and Western blotting. Furthermore, LY294002, a selective PI3K/AKT inhibitor, significantly attenuated the protective effects of 7-HEC against HAPE.

Conclusion: These findings indicate that 7-HEC may mitigate HAPE by activating the PI3K/AKT signaling pathway and could serve as an effective agent for preventing HAPE.

Keywords: 7-hydroxyethyl chrysin, high-altitude pulmonary edema, oxidative stress, inflammatory response, endothelial function, PI3K/AKT signaling pathway

Introduction

High altitude pulmonary edema (HAPE) is a grievous, life-threatening acute mountain sickness that mainly occurs during rapid ascent to high altitude in people who have not been acclimatized to high altitude environments.[1] HAPE manifests as conspicuous dyspnoea, extreme fatigue, and exercise intolerance, accompanied by chest tightness, cyanosis, and cough with pink frothy sputum.[2] The incidence of HAPE is generally about 0.5–1.0% and without effective treatment, the mortality rate can be as high as 50%.[3] HAPE received growing concern due to the fact that millions of people travel to high-altitude regions each year for work, leisure, and adventure.[4]

Limiting the rate of ascent, supplemental oxygen, and rapid passive descent to the lowest possible altitude are effective measures for prevention and treatment of HAPE.[5] In addition, appropriate pharmacological therapy is required. At present, the drugs used for preventing and treating of HAPE include nifedipine, sildenafil, salmeterol, acetazolamide,

Received: 10 June 2025
Accepted: 27 November 2025
Published: 10 December 2025

and dexamethasone.[6] However, these drugs have obvious side effects.[7–10] Hence, developing novel, safe, effective, and economical drugs for the treatment of HAPE are urgently needed.

Although the precise mechanisms underlying HAPE remain incompletely understood, it is widely acknowledged that overproduced free radical-mediated oxidative stress and inflammation response under hypobaric hypoxia (HH) conditions are two key factors in the development of HAPE,[11,12] which raises the possibility that anti-oxidative and anti-inflammatory drugs may help prevent HAPE.

7-hydroxyethyl chrysin (7-HEC, Figure 1) is a derivative obtained by hydroxyethylation of the hydroxyl group at position 7 of chrysin. Compared with chrysin, the solubility of 7-HEC was significantly improved (Table S1). Our previous studies have found that 7-HEC can significantly improve HH-induced brain tissue damage[13] and cognitive dysfunction[14] in rats, as well as alleviate hypoxia-induced nerve and myocardial cell damage.[15,16] However, its protective effect on HAPE is still unclear. Therefore, in this study, we aimed to assess the protective effect of 7-HEC against HAPE using a rat mode for the first time.

Materials and Methods

Chemicals and Regents

7-HEC (HPLC purity > 98%) was synthesized in our laboratory.[17] Acetazolamide (ACZ, Lot No. S-20110104, HPLC purity > 99%) was obtained by Wuhan Yuancheng Technology Development Co.,Ltd. Protein ladder (catalogue No. 26616) were provided by Thermo Fisher Scientific. Other reagents were described in Table S2.

Construction of Networks

The SwissTargetPrediction (http://www.swisstargetprediction.ch/), Similarity ensemble approach (https://sea.bkslab.org/), and SuperPred (https://prediction.charite.de/) databases were used to retrieve the potential targets of 7-HEC. The search term "high altitude pulmonary edema" was used to query the GeneCards (https://www.genecards.org/) and OMIM (https://www.omim.org/) databases to identify HAPE-related targets. The intersection targets between 7-HEC and HAPE were obtained and visualized by Venny 2.1. Then those overlapped targets were used for protein–protein interaction (PPI) analysis by importing into the STRING (https://string-db.org) database. Cytoscape 3.9.1 was used to visualize the results and identified the hub targets. This study, which involved analysis of publicly available datasets, was exempt from ethics committee approval in accordance with Items 1 and 2 of Article 32 of the Measures for Ethical Review of Life Science and Medical Research Involving Human Subjects (National Health Commission of China, issued February 18, 2023).

Gene Ontology (GO) and Kyoto Encyclopedia of Genes and Genomes (KEGG) Pathway Enrichment Analysis

To elucidate the potential targets of 7-HEC against HAPE, DAVID database (https://david.ncifcrf.gov/) was utilized for GO and KEGG enrichment analyses of the overlapped targets. Then, visualization was carried out using online platform https://www.bioinformatics.com.cn.[18]

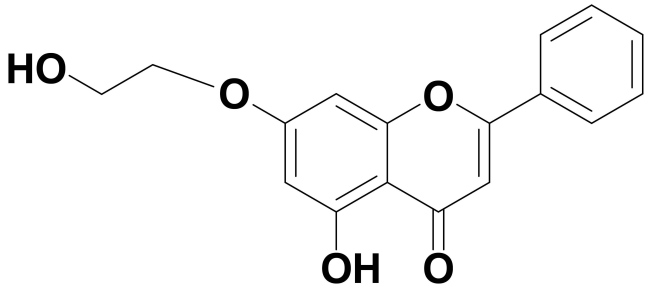

Figure 1 Chemical structure of 7-HEC.

Molecular Docking

The potential binding mode of 7-HEC to hub targets was investigated through molecular docking analysis. The three-dimensional (3D) structure of 7-HEC was obtained using ChemBio3D Ultra software. The 3D structures of the target proteins were downloaded from the Protein Data Bank (PDB, http://www.rcsb.org) and appropriately modified using PyMOL software. AutoDock Vina software was used to dock the 7-HEC to the receptor proteins. The molecular docking range parameters are detailed in Table S3. The docking results were visualized using PyMOL amd Discovery studio software.

Animal

Specific pathogen-free (SPF) male BALB/c mice weighing 18–22 g were provided by Laboratory Animal Center of Lanzhou University. SPF male Wistar rats weighing 180–220 g (6–8 weeks old) were provided by Laboratory Animal Center of Gansu University of Traditional Chinese Medicine. Animals were housed in a SPF room with controlled environment (temperature, 22 °C, humidity, 50% and 12-hour light/dark cycle) and free access to food and water. The adaptation period was five days before the start of the experiment. All animal experiments were approved by the Animal Care and Use Committee of 940th Hospital of Joint Logistics Support Force of PLA (Approval no. 2015GKT017) and conducted following by the National Research Council's Guide for the Care and Use of Laboratory Animals.

Normobaric Hypoxia Test

50 mice were randomized into into five groups (ten mice per group): hypoxia group, acetazolamide group (250 mg/kg), and three 7-HEC groups (125, 250 or 500 mg/kg). Acetazolamide, which has been proven effective against HAPE, was utilized as a positive drug.[19] Both compounds were suspended in normal saline containing 5% Tween 80. Mice were administered acetazolamide or 7-HEC via oral gavage once daily for five days. The mice in the hypoxia group were administered with normal saline containing 5% Tween 80 (0.2 mL/20 g) via gavage once daily for five days. Thirty minutes after the last administration, the normobaric hypoxia test was conducted according to our previously reported method. The survival time and the prolongation rate were recorded.

Acute Decompression Hypoxia Tolerance Test

100 mice were randomized into five groups (twenty mice per group): acute decompression group (normal saline, 0.2 mL/20 g), acetazolamide group (250 mg/kg), and three 7-HEC groups (125, 250 or 500 mg/kg). After drug administration as described above, the mice were placed in a FLYDMC50-IIC hypobaric hypoxia cabin (Guizhou FengLei, China). The decompression rate was set at 20 m/s. The altitude was first increased to 5000 m and held for 5 minutes, then to 8000 m and held for 5 minutes, and finally to 10,000 m and held for 1 hour. The survival rate was counted.

Establishment of HAPE Rats Model and Drug Administration

Rat model of HAPE was replicated according to our recently reported method.[20] 80 rats were randomized into four groups: Control (Con) group, HAPE group, HAPE+acetazolamide (HAPE+ACZ, 250 mg/kg) group, and HAPE+7-HEC (350 mg/kg) group. Drugs was given via oral gavage for six consecutive days. The doses of 7-HEC was selected based on the results of the normobaric hypoxia and the acute decompression experiments.

To explore the mechanism of PI3K/AKT signaling pathway on HAPE mice, 48 rats were randomly divided into four groups: HAPE group, HHBI+LY group (LY294002 intervention group, 10 mg/kg), HAPE+7-HEC group (7-HEC intervention group, 350 mg/kg), and HAPE+7-HEC+LY group (LY294002 intervention before 7-HEC treatment). LY294002 was dissolved in saline containing 5% dimethyl sulfoxide and administered via intraperitoneal injection (0.2 mL/kg) for six consecutive days.

Samples Preparation

Rats were anesthetized at a simulated altitude of 4000 m in the hypobaric hypoxia cabin. Blood was drawn from the abdominal aorta, after which the rats were sacrificed and the lungs were removed.

Arterial Blood Gas Measurements

Polypropylene syringes containing heparin was used to draw blood from the abdominal aorta. Partial pressure of oxygen (PaO_2), partial pressure of carbon dioxide ($PaCO_2$), oxygen saturation in arterial blood (SaO_2), pH, blood bicarbonate (HCO_3^-), lactic acid (Lac), sodium (Na^+), potassium (K^+), and calcium (Ca^{2+}) were rapidly measured using a blood gas analyzer (pHOx Plus L, Nova Biomedical, Flintshire, UK).

Routine Blood Examination

Blood was drawn from the abdominal aorta into K2 EDTA vacuum tubes and used for routine blood examination. White blood cell (WBC), red blood cell (RBC), hemoglobin (HGB), platelet count (PLT), Neutrophil (NEUT), and lymphocyte (LYM) were assessed using an automated hematology analyzer (XT-2000i, SYSMEX, Japan).

Lung Water Content (LWC)

To evaluate the severity of pulmonary edema, LWC was calculated. The wet weight of left lung was first recorded. The lung tissue was then placed in an oven at 80 °C and dried for 72 hours until a constant weigh was achieved, after which the dry weight was recorded. Finally, LWC was calculated according to the equation: LWC (%) = (1 - dry weight/wet weight) ×100%.

Pulmonary Microvascular Permeability Test

Pulmonary microvascular permeability was determined by measuring extravasated Evans blue (EB) dye.[21] In brief, rats are injected with 1% EB solution (2 mL/kg) through the tail vein. 30 minutes later, the lungs were perfused with saline through the right ventricle until colorless fluid flowed out of the left atrium to remove the dye in the blood vessels. The right lung was harvested, washed three times with cold saline, and blotted dry with filter paper. The tissue was weighed, cut into small pieces, and EB was extracted using formamide. The supernatant was collected, and the absorbance at 620 nm was recorded. The blank control solution was an equal volume of formamide. EB content was calculated using a linear standard curve and expressed as μg of EB per gram of lung tissue.

Hematoxylin and Eosin (HE) Staining

Freshly harvested lung tissues were fixed using 4% paraformaldehyde solution for 24 hours. Subsequently it was paraffin-embedded, sectioned into 5-μm thick slices, and stained with the hematoxylin and eosin. An optical microscope (Nikon, Japan) was employed to capture the images.

Determination of Biochemical Indexes in Lung Tissue

Rat lung tissues were homogenized in normal saline at 4 °C, centrifuged, and the supernatant was collected for subsequent analysis. A BCA kit was used to determine the total protein content. The contents of hydrogen peroxide (H_2O_2), malonaldehyde (MDA), glutathione (GSH), lactate (LD) and pyruvate, as well as the activities of superoxide dismutase (SOD), catalase (CAT), glutathione peroxidase (GSH-Px), myeloperoxidase (MPO), glutathione S-transferases (GST), total antioxidant capacity (T-AOC), lactate dehydrogenase (LDH), pyruvate kinase (PK), and ATPase were determined using related kits according to the instructions.

Enzyme-Linked Immunosorbent Assay (ELISA)

Blood was drawn from the abdominal aorta into vacuum tubes and allowed to left at room temperature for 30 minutes. Serum was obtained by centrifugation for 10 minutes at 3500 rpm. The concentrations of tumor necrosis factor alpha (TNF-α), interleukin-1β (IL-1β), and interleukin-6 (IL-6) in serum, as well as the contents of nitric oxide (NO), endothelin-1 (ET-1), soluble vascular cell adhesion molecule-1 (sVCAM-1), and soluble intercellular adhesion molecule-1 (slCAM-1) in lung tissue were measured using ELISA kits according to the instructions.

Quantitative Real-Time Polymerase Chain Reaction (qRT-PCR)

Total ribonucleic acid (RNA) was extracted from lung tissue using the MiniBEST Universal RNA Extraction Kit (TakaRa, Japan). Subsequently, cDNA reverse kit (Cat #AK3502, TakaRa, Japan) was used for complementary DNA (cDNA) synthesis following by the manufacturer's instructions. qRT-PCR was conducted on a ViiA7 Dx Real-Time system (Applied Biosystems, USA) using 2× SYBR Premix Ex Taq^{TM} II (Cat #AK8106, TakaRa, Japan). The relative expression levels of gene were normalised to GAPDH using the $2^{-\Delta\Delta CT}$ method. The primer sequences were listed below: HIF-1α rats (forward primer: TCTAGTGAACAGGATGGAATGGAG, reverse primer: TCGTAACTGGTCAGCTGTGGTAA) VEGFA rats (forward primer: TCCTGCAGCATAGCAGATGTGA, reverse primer: CCAGGATTTAAACCGGGATTTC), Occludin rats (forward primer: GTCTTGGGAGCCTTGACATCTTG, reverse primer: GCATTGGTCGAACGTGCATC), α-ENaC rats (forward primer: ACGGAGTTGCAAAGCTCAACATC, reverse primer: AGCCAAACCACAGGCTCCAC), AQP1 (forward primer: GACTACACTGGCTGTGGGATCAA, reverse primer: CCAGGGCACTCCCAATGAA), NF-kB p65 rats (forward primer: CGCAAAAGGACCTACGAGAC, reverse primer: TGGGGGAAAACTCATCAAAG), GAPDH (forward primer: GGCACAGTCAAGGCTGAGAATG, reverse primer: ATGGTGGTGAAGACGCCAGTA).

Western Blotting

Proteins were separated from the lung tissue using RIPA buffer. A BCA assay kit was used for measurement of protein concentration. After being separated on sodium dodecyl sulfate-polyacrylamide gel electrophoresis (SDS-PAGE) gels, the proteins were placed onto Polyvinylidene Fluoride (PVDF) membranes. The membranes were blocked with 5% nonfat milk for 2 hours and incubated with primary antibodies overnight at 4 °C, followed by incubation with secondary antibodies at room temperature for 1 hour. Protein bands were visualized with a ChemiDoc" MP lmaging System (BIO-RAD, USA). The intensities of protein bands were analyzed using ImageJ software (Madison, WI, USA) by normalizing to β-actin.

Statistical Analysis

The measurement data were represented as mean ± standard deviation (SD). GraphPad Prism 8.0 software was used for statistical analysis and generation of graphs. For comparisons between two groups, the Student's *t*-test was performed. For multiple-group comparisons, one-way analysis of variance (ANOVA) following by Tukey's tests or Dunnett's test were performed. Fisher's exact test and Chi-square test were performed to assess survival differences. $P < 0.05$ denoted statistical significance.

Results

7-HEC Extended the Survive Time of Mice in Normobaric Hypoxia Test

To evaluate the anti-hypoxic efficacy of 7-HEC, we first performed the normobaric hypoxia test. As seen in Table 1, 7-HEC administration dose dependently extended the survival time of mice exposed to hypoxia environment ($P < 0.01$ or $P < 0.05$). The prolongation rates of mice in the low, medium, and high dose 7-HEC groups were 16.56%, 28.19%, and

Table 1 Effect of 7-HEC on the Survival Time of Mice in the Normobaric Hypoxia Test (X±s, n=10)

Group	Dose (mg/kg)	Survival Time (min)	Prolongation Rate (%)
Hypoxia group	–	30.80±0.91	–
Acetazolamide group	250	37.75±2.59*	22.56
7-HEC group	125	35.90±2.10*	16.56
	250	39.48±1.81**	28.19
	500	47.07±4.29**	52.84

Note: Data are expressed as mean ± SD or percent (%). *$P < 0.05$, **$P < 0.01$ vs Hypoxia group. Prolongation rate (%) = (survival time of treatment group/survival time of hypoxia group - 1) ×100.

https://doi.org/10.2147/DDDT.S541390

52.84%, respectively. ACZ treatment also significantly prolonged the survival time of mice with a prolongation rate of 22.56%. These results demonstrate that 7-HEC exhibits excellent anti-hypoxic activity.

7-HEC Elevated the Survive Rate of Mice in Acute Decompression Hypoxia Tolerance Test

We further assessed the protective effect of 7-HEC under HH conditions using the acute decompression model. As seen in Table 2, ACZ intervention significantly elevated the survival rate of mice under acute decompression condition from 15% to 25%. Treatment with 7-HEC at doses of 125, 250 and 500 mg/kg also elevated the survival rates to 35%, 40%, and 50%, respectively. The higher survival time and survival rate, the stronger the anti-hypoxic activity. These results indicated that 7-HEC could improve the hypoxia tolerance of mice. High dose of 7-HEC exhibited the best effect. Therefore, through dose translation between laboratory animals, the dose of 350 mg/kg was chosen for assessing the protective effect of 7-HEC on HAPE in rats. The schematic diagram of the experimental protocols used in this study was shown in Figure 2A.

7-HEC Decreased the Lung Water Content (LWC) of HAPE Rats

We next examined whether 7-HEC could alleviate pulmonary edema in HAPE rats. As can be seen from Figure 2B, compared with the Con group, the LWC of rats in HAPE group was notably elevated ($P < 0.01$). Compared with the HAPE group, the LWC of rats in ACZ and 7-HEC groups was significantly reduced ($P < 0.01$). This indicates that 7-HEC effectively attenuates pulmonary edema in HAPE rats.

7-HEC Decreased the Pulmonary Microvascular Permeability of HAPE Rats

To further assess the protective effect of 7-HEC against HAPE, we also measured pulmonary microvascular permeability using Evans blue extravasation. As can be seen from Figure 2C, compared with the Con group, EB content in the lung tissue of rats in HAPE group was notably elevated ($P < 0.01$). Compared with the HAPE group, 7-HEC treatment significantly lowered the EB content in lung tissue of rats ($P < 0.01$), while ACZ administration also decreased the EB content, though not significantly. These results suggest that 7-HEC significantly stabilizes vascular endothelial integrity under HH conditions.

7-HEC Improved Pathological Alterations of Lung Tissue in HAPE Rats

To evaluate the histological impact of 7-HEC, lung tissue pathology was examined. As can be seen from Figure 2D, the lung tissue structure was normal with no obvious pathological change in the Con group. In the HAPE group, lung interstitium and alveolar wall were notably thickened, accompanied by substantial inflammatory cell infiltration and edema. Compared to the HAPE group, both ACZ and 7-HEC treatments remarkably improved alveolar wall thickening, maintained the integrity of alveolar space structure, relieved alveolar edema, and reduced inflammatory cell infiltration. These results indicate that 7-HEC effectively attenuates HAPE-induced lung tissue injury.

Table 2 Effect of 7-HEC on the Survival Rate of Mice in the Acute Decompression Hypoxia Test (X±s, n=20)

Group	Dose (mg/kg)	Number of Deaths (Single)	Survival Rate (%)
Acute decompression group	-	17	15
Acetazolamide group	200	15	25*
	25	13	35*
7-HEC group	50	12	40*
	100	10	50**

Notes: Data are expressed as percent (%). *$P < 0.05$, **$P < 0.01$ vs Acute decompression group. The data of mortality rates were analyzed by Fisher's exact test and Chi-square test.

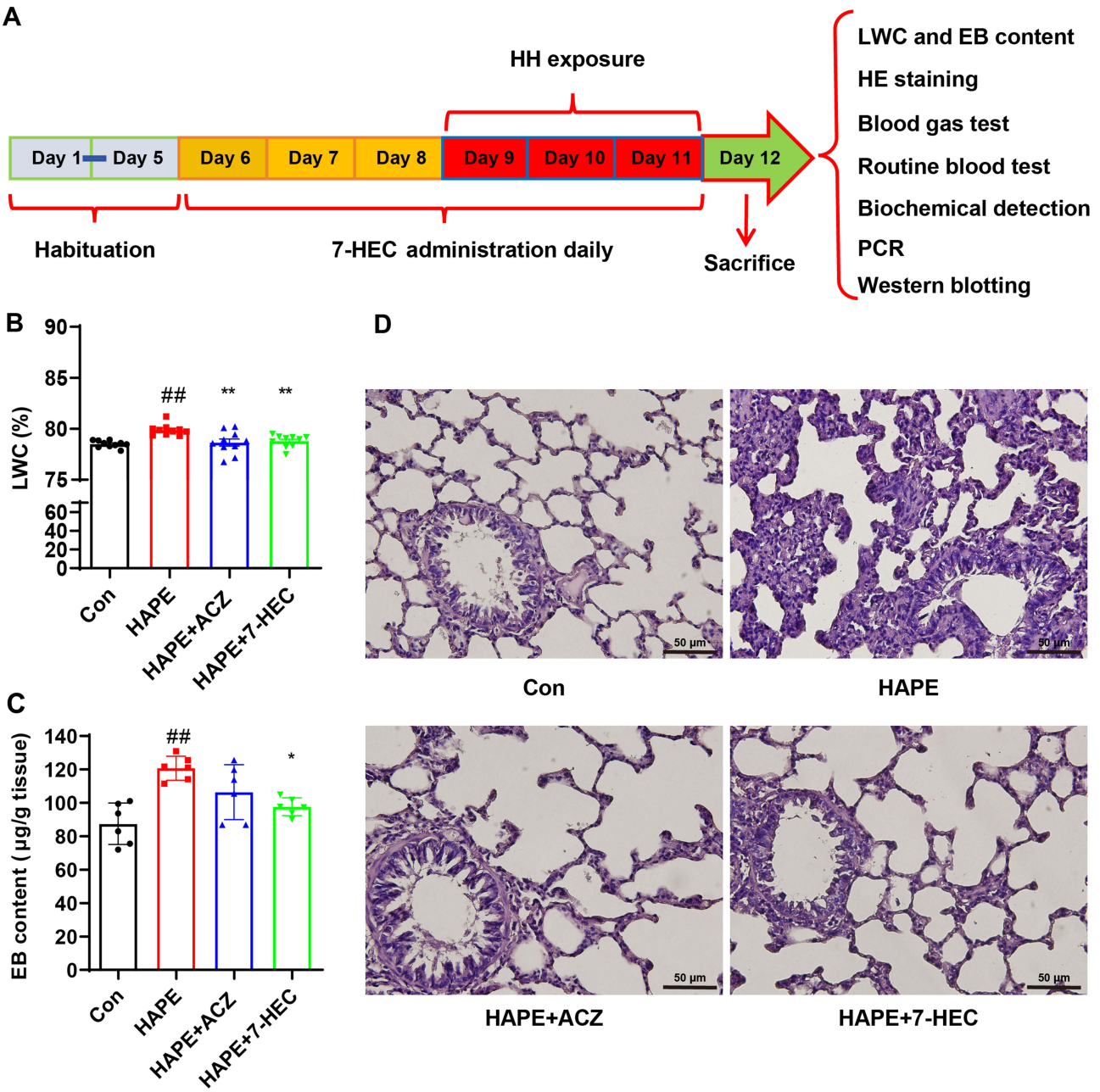

Figure 2 Effect of 7-HEC against HAPE. (**A**) Schematic diagram of the experimental protocols used in this study. (**B**) Lung water content. (**C**) EB leakage. Data are presented as mean ± SD (n = 10 or 6). $^{\#\#}P < 0.01$ vs Con group; $^{*}P < 0.05$, $^{**}P < 0.01$ vs HAPE group. (**D**) Histopathological changes of lung tissues observed by HE staining. Scale bar: 50 μm.

7-HEC Improved Lung Permeability of HAPE Rats via Regulating Related Genes and Proteins

We further investigated the molecular mechanisms underlying 7-HEC's protective effects on lung barrier function. As can be seen from Figure 3A–E, the expressions of HIF-1α and VEGF mRNA were notably up-regulated ($P < 0.01$), while the expressions of Occludin, AQP1 and α-ENaC mRNA were notably down-regulated ($P < 0.01$) in the HAPE group, compared with the Con group. Treatment with ACZ and 7-HEC significantly reduced the expressions of HIF-1α and VEGF mRNA, while elevated the expressions of Occludin, AQP1 and α-ENaC mRNA ($P < 0.01$ or $P < 0.05$), compared with the HAPE group. Consistently, as can be seen from Figure 3F–I, compared with the Con group, the protein expressions of VEGF were notably up-regulated ($P < 0.05$), while the protein expressions of Occludin and AQP1 were

https://doi.org/10.2147/DDDT.S541390

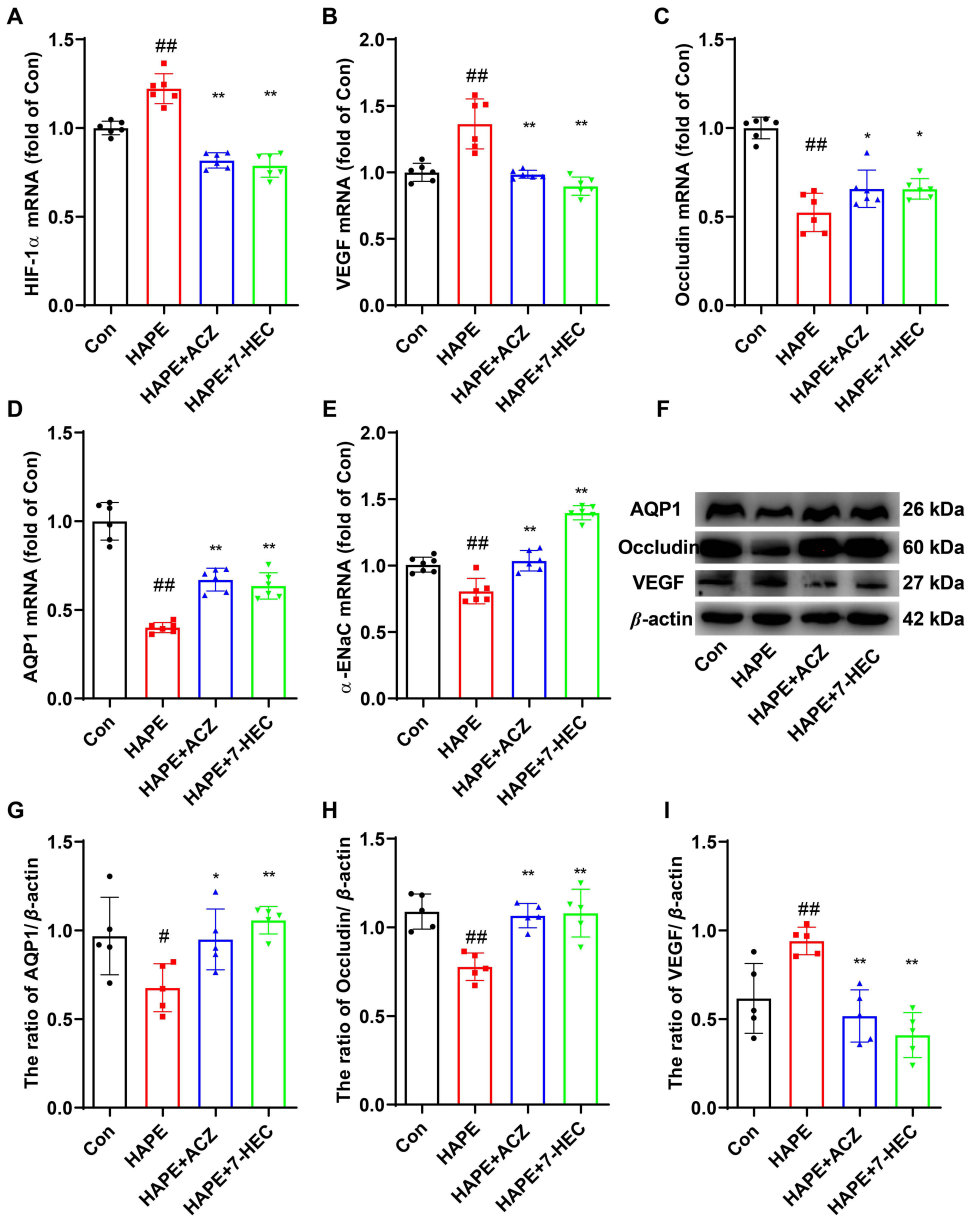

Figure 3 Effect of 7-HEC on permeability in the lung tissue of HAPE rats. Relative mRNA expression of HIF-1α (**A**), VEGF (**B**), Occludin (**C**), AQP1 (**D**), αENa (**E**). GAPDH was used as a loading control. (**F**) Representative Western blot analysis of AQP1, Occludin and VEGF. Quantification of the expression of AQP1 (**G**), Occludin (**H**), and VEGF (**I**). Data are presented as mean ± SD (n = 5 or 6). $^{\#}P < 0.05$, $^{\#\#}P < 0.01$ vs Con group; $^{*}P < 0.05$, $^{**}P < 0.01$ vs HAPE group.

notably down-regulated in the HAPE group. Treatment with ACZ and 7-HEC also remarkably reversed these changes ($P < 0.01$ or $P < 0.05$). These data demonstrate that 7-HEC restores lung permeability through regulation of key barrier-related genes and proteins.

7-HEC Improved the Arterial Blood Gas Indexes of HAPE Rats

We next assessed whether 7-HEC ameliorates hypoxemia and metabolic imbalance in HAPE rats. As can be seen from Figure 4A–E, PaO_2, $PaCO_2$, SaO_2, pH, HCO_3^- was significantly elevated in HAPE rats, compared to the Con group ($P < 0.01$). ACZ and 7-HEC treatment significantly downregulated the above indicators. As can be seen from Figure 4F–I, compared with the Con group, the contents Lac, Na^+, and K^+ were significantly decreased, while Ca^{2+} content was significantly increased in the HAPE group. ACZ and 7-HEC treatment notably reversed these changes ($P < 0.01$ or $P < 0.05$). These results suggest that 7-HEC helps restore blood gas homeostasis and electrolyte balance in HAPE rats.

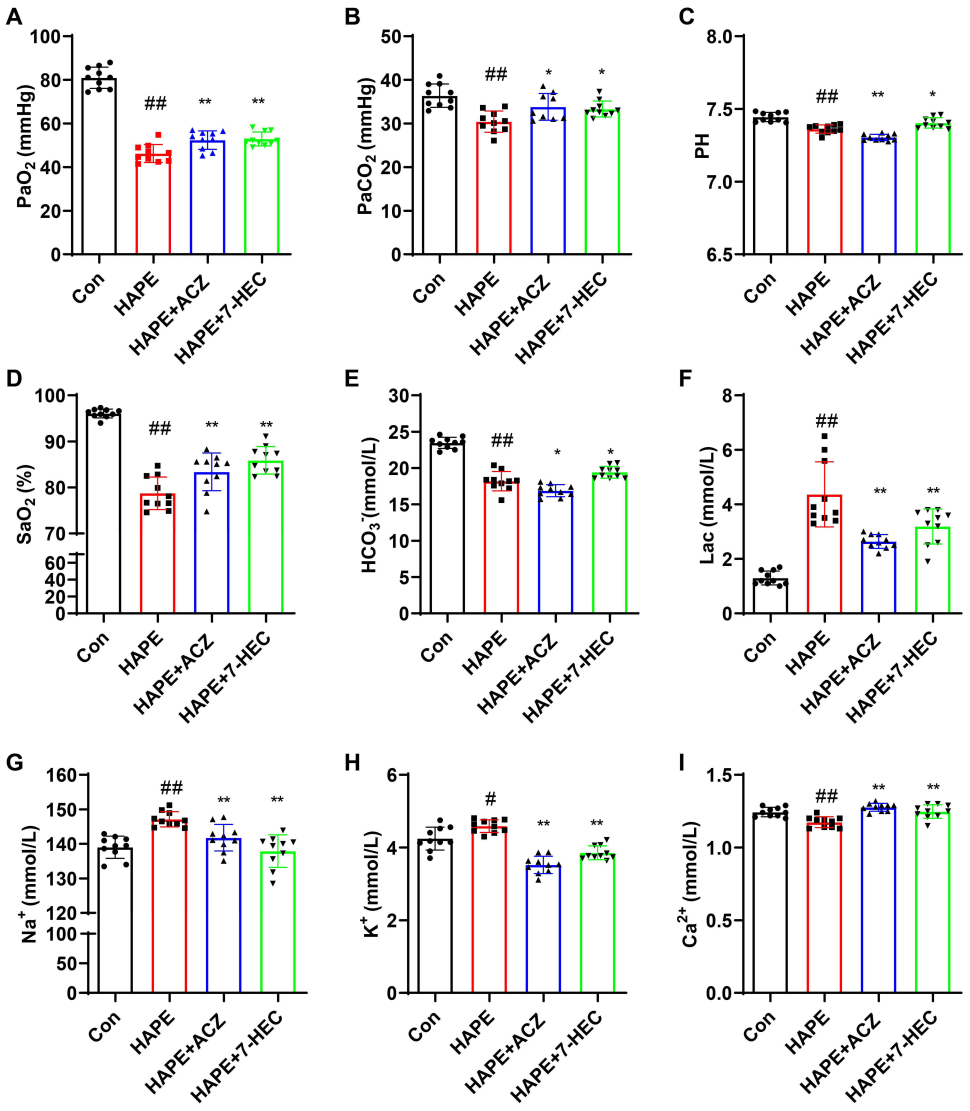

Figure 4 Effect of 7-HEC on arterial blood gas in HAPE rats. (**A**) PaO_2, (**B**) $PaCO_2$, (**C**) PH, (**D**) SaO_2, (**E**) HCO_3^-content, (**F**) Lac content, (**G**) Na^+ content, (**H**) K^+ content, (**I**) Ca^{2+} content. Data are presented as mean ± SD (n = 6). $^{\#}P < 0.05$, $^{\#\#}P < 0.01$ vs Con group; $^{*}P < 0.05$, $^{**}P < 0.01$ vs HAPE group.

7-HEC Improved the Routine Blood Indexes of HAPE Rats

To determine the effect of 7-HEC on systemic hematological responses, routine blood parameters were analyzed. As can be seen from Figure 5A–F, levels of WBC, RBC, HGB, PLT, NEUT, and LYM were significantly elevated in the HAPC group ($P < 0.01$), compared to the Con group. Treatment with ACZ and 7-HEC restored these indexes to the normal level ($P < 0.01$ or $P < 0.05$). These results indicate that 7-HEC mitigates HAPE-associated abnormal hematological changes.

7-HEC Suppressed the Pulmonary Oxidative Stress of HAPE Rats

To determine the effect of 7-HEC on oxidative stress, we measured key biomarkers in lung tissue. As can be seen from Figure 6A–I, compared to the Con group, the contents of H_2O_2, MDA and the activity of MPO were significantly elevated, while the activities of SOD, CAT, GSH-Px, GST, and T-AOC, as well as the level of GSH were significantly reduced in the HAPE group ($P < 0.01$). Treatment with 7-HEC notably reversed these changes ($P < 0.01$ or $P < 0.05$). ACZ also significantly ameliorated most oxidative stress markers, although its effects on GSH and MPO were not statistically significant. These results demonstrate that 7-HEC effectively attenuates HAPE-induced pulmonary oxidative stress.

https://doi.org/10.2147/DDDT.S541390

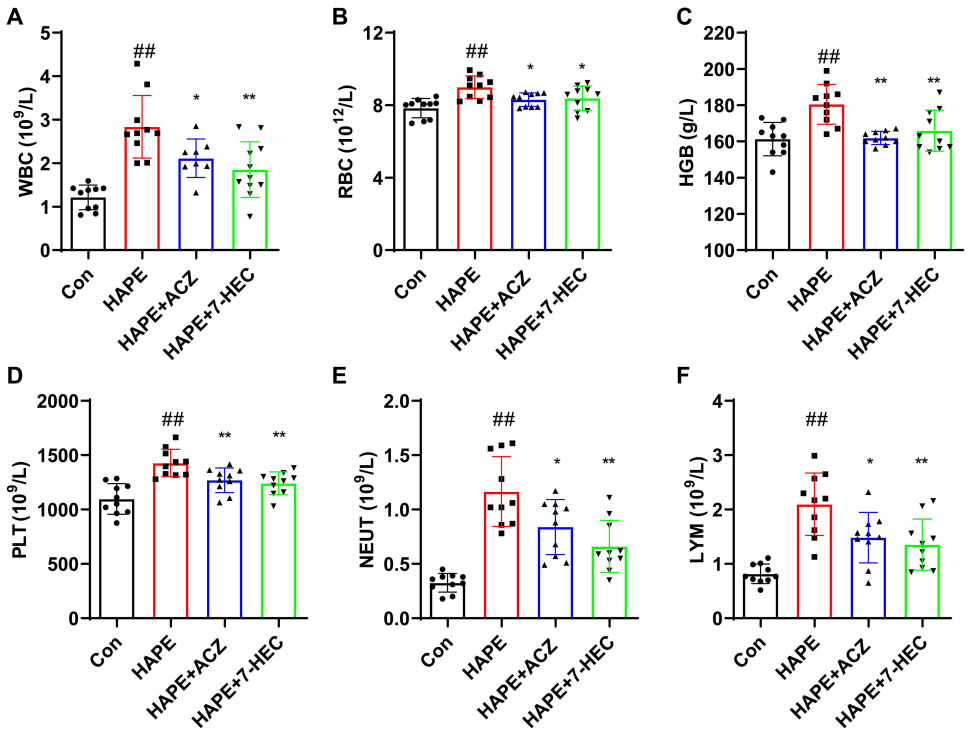

Figure 5 Effect of 7-HEC on routine blood indexes in HAPE rats. (**A**) WBC, (**B**) RBC, (**C**) HGB, (**D**) PLT, (**E**) NEUT, (**F**) LYM. Data are presented as mean ± SD (n = 6). $^{\#\#}P < 0.01$ vs con group; $^{*}P < 0.05$, $^{**}P < 0.01$ vs HAPE group.

7-HEC Suppressed the Inflammation Response of HAPE Rats

We next evaluated whether 7-HEC modulates the inflammatory cascade in HAPE rats. As can be seen from Figure 7A–C, the serum levels of TNF-α, IL-1β, and IL-6 in HAPE rats were significantly higher than those in the Con rats, whereas ACZ and 7-HEC treatment reversed these changes. Furthermore, elevated NF-κB p65 mRNA expression and increased p-NF-κB p65/NF-κB p65 ratio were observed in the lung tissue of HAPE rats, changes that were significantly reversed by ACZ and 7-HEC treatment (Figure 7D–F, $P < 0.01$ or $P < 0.05$). These findings indicate that 7-HEC mitigates HAPE-related inflammation likely through suppression of the NF-κB pathway.

7-HEC Suppressed the Pulmonary Energy Metabolism Dysfunction of HAPE Rats

We further investigated the influence of 7-HEC on cellular energy metabolism in the lung. As can be seen from Figure 8A–G, the contents of LD and PA, as well as the activities of LDH and PK were significantly elevated, while the ATP content and ATPase activities were significantly reduced in the lung tissue of HAPE rats, compared to the Con group. 7-HEC treatment reversed these changes. ACZ treatment also remarkably lowered the levels of LD, LDH, PK, and PA ($P < 0.01$ or $P < 0.05$), while had no significant role on the levels of ATP and ATPase. These results suggest that 7-HEC helps restore energetic homeostasis in the lung tissue of HAPE rats.

7-HEC Suppressed the Pulmonary Endothelial Dysfunction of HAPE Rats

To assess vascular endothelial function, we measured relevant mediators in lung tissue. As can be seen from Figure 9A–E, the levels of NO and eNOS in lung tissue were notably reduced ($P < 0.01$), while the contents of ET-1, sVCAM-1, and slCAM-1 in lung tissue were notably elevated ($P < 0.01$) in the HAPE group, compared to the Con group. Treatment with ACZ and 7-HEC remarkably reversed these changes ($P < 0.01$ or $P < 0.05$). These results suggest that 7-HEC protects against HAPE-induced endothelial dysfunction by restoring the balance of vasoactive and adhesion molecules.

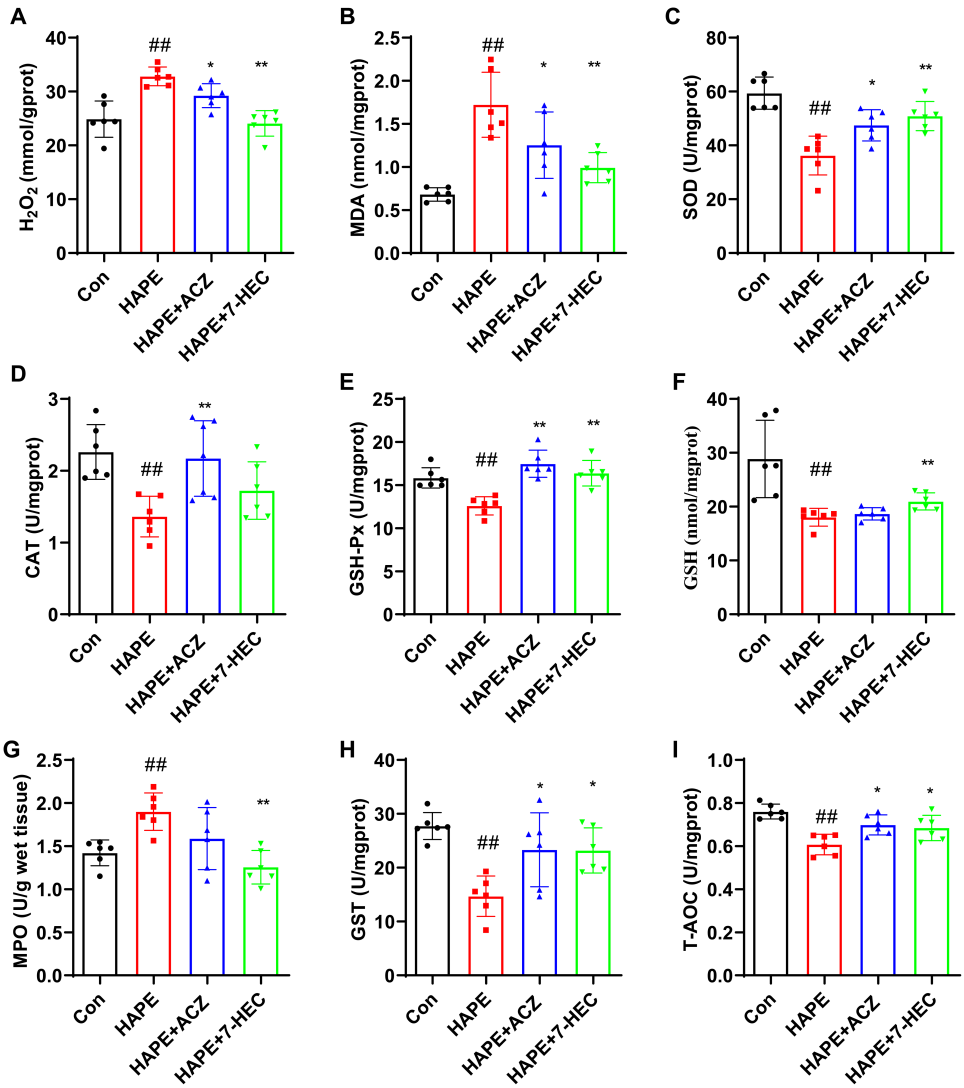

Figure 6 Effect of 7-HEC on oxidative stress in the lung tissue of HAPE rats. (**A**) H_2O_2 content, (**B**) MDA content, (**C**) SOD activity, (**D**) CAT activity, (**E**) GSH-Px activity, (**F**) GSH content, (**G**) MPO activity. (**H**) GST activity. (**I**) T-AOC. Data are presented as mean ± SD (n = 6). $^{\#\#}P < 0.01$ vs Con group; $^{*}P < 0.05$, $^{**}P < 0.01$ vs HAPE group.

Potential Targets of HAPC and 7-HEC

To identify potential therapeutic targets, we performed a comprehensive database screening. As illustrated in Figure 10A, a total of 220 targets of 7-HEC were collected from the Similarity ensemble approach, SuperPred and Swiss Target prediction databases, and a total of 967 targets of HAPE were collected from Genecards and OMIM databases. 38 intersecting targets were identified, indicating that 7-HEC may treat HAPE through these targets.

PPI Network Construction and Hub Targets Selection

To further understand the functional interactions among the overlapping targets, a PPI network was constructed using the STRING database and Cytoscape software. This network contained 38 nodes and 231 edges (Figure 10B and C). Hub genes were consistently identified via three algorithms (Degree, Closeness, and MCC) of CytoHubba and MCODE (Figure 10D). The top hub targets based on algorithm scores were TNF, EGFR, HIF1A, HSP90AA1, MMP9, ESR1, NFKB1, PPARG, and HSP90AB1 (Figure 10E and Table 3).

https://doi.org/10.2147/DDDT.S541390

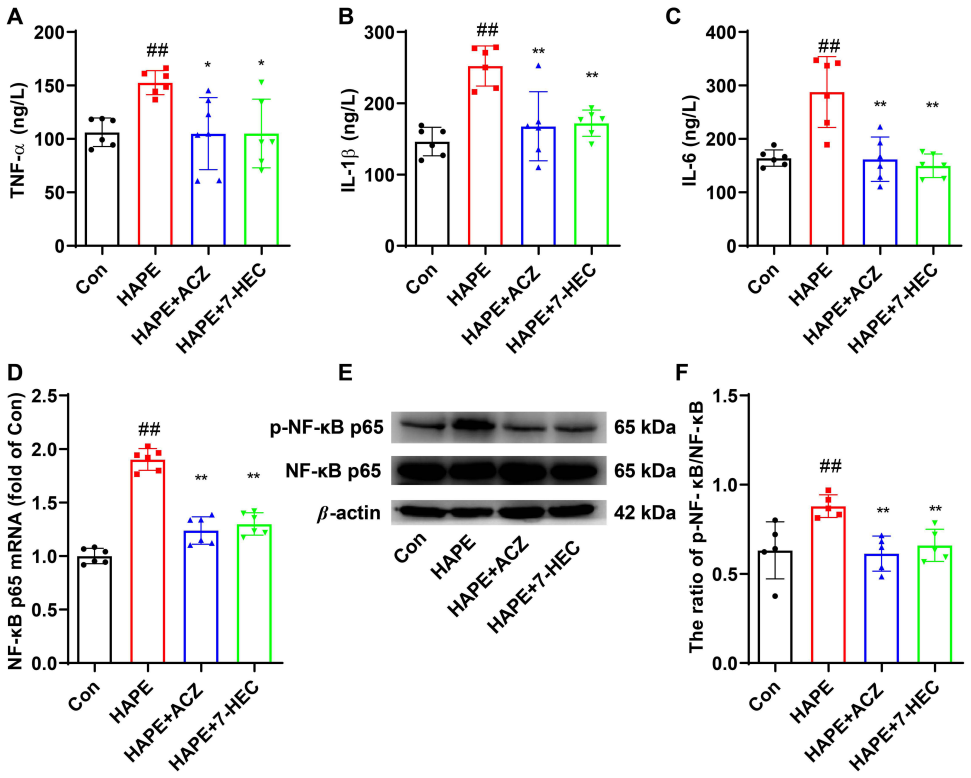

Figure 7 Effect of 7-HEC on inflammatory response in HAPE rats. (**A**) TNF-α content in serum, (**B**) IL-1β content in serum, (**C**) IL-6 content in serum, (**D**) Relative mRNA expression of NF-κB in lung tissue, (**E**) Representative Western blot analysis of p-NF-κB and NF-κB in lung tissue, (**F**) Ratio of p-NF-κB/NF-κB in lung tissue. Data are presented as mean ± SD (n = 5 or 6). $^{\#\#}P < 0.01$ vs Con group; $^{*}P < 0.05$, $^{**}P < 0.01$ vs HAPE group.

Molecular Docking Verification

To validate the binding interactions between 7-HEC and the hub targets, molecular docking was performed. The free energy of binding between 7-HEC and all nine hub targets (TNF, EGFR, HIF1A, HSP90AA1, MMP9, ESR1, NFKB1, PPARG, and HSP90AB1) was less than −6 kcal/mol, indicating strong binding affinity (Table 4). The binding sites between 7-HEC and hub targets were depicted in Figure 10F. These results confirm a high affinity between 7-HEC and the core targets.

GO and KEGG Enrichment Analyses

To obtain a more detailed understanding of the potential mechanisms of 7-HEC against HAPE, GO and KEGG enrichment analyses were performed on the 38 key targets. GO annotation (Figure 11A) showed that the 38 key targets were classified into 176 biological processes (BP) terms, mainly associated with negative regulation of apoptotic process, response to hypoxia and inflammatory response; 32 cellular components (CC) terms, mainly located in the plasma membrane, cytosol, cytoplasm, and nucleus; and 80 molecular function (MF) terms, mainly related to protein binding, enzyme binding, ATP binding, and DNA binding.

KEGG pathway analysis showed that 38 key targets were classified into 54 KEGG pathways. As shown in Figure 11B, the targets were predominantly associated with PI3K/AKT signaling pathway, HIF-1 signaling pathway, Chemical carcinogenesis-reactive oxygen species, and MAPK signaling pathway. Notably, these signaling pathways related to oxidative stress and inflammatory response. Among them, PI3K/AKT signaling pathway had the highest number of targets. In addition, three hub genes related to PI3K/AKT signaling pathway, such as NFKB1, EGFR, and HSP90AB1 participated in the greatest number of pathways (Figure 11C). Therefore, we plotted the PI3K-AKT signaling pathway diagram[22] using the red box to indicate the key targets (Figure 11D).

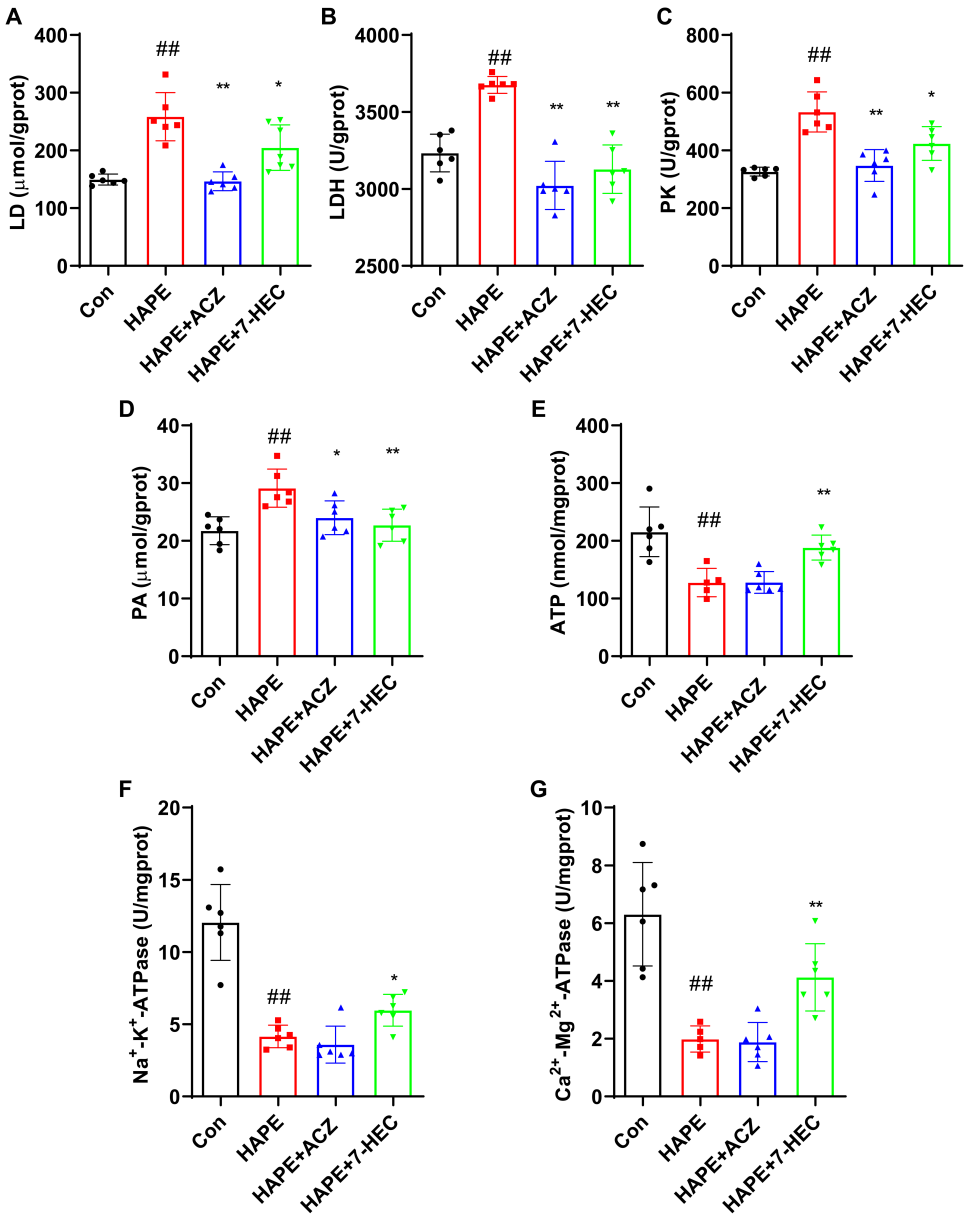

Figure 8 Effect of 7-HEC on energetic metabolism in the lung tissue of HAPE rats. (**A**) LD content. (**B**) LDH activity, (**C**) PK activity, (**D**) Pyruvate content, (**E**) ATP content, (**F**) Na^+-K^+-ATPase activity, (**G**) Ca^{2+}-Mg^{2+}-ATPase activity. Data are presented as mean ± SD (n = 6). $^{\#\#}P < 0.01$ vs Con group; $^{*}p < 0.05$, $^{**}P < 0.01$ vs HAPE group.

7-HEC Reversed the Inhibition of the PI3K/AKT Signaling Pathway of HAPE Rats

We further validated the regulatory effect of 7-HEC on the PI3K/AKT signaling pathway in vivo. As can be seen from Figure 12A–C, the ratios of p-PI3K/PI3K and p-AKT/AKT in the lung tissue of HAPE rats were significantly decreased compared to that in control rats ($P < 0.01$ or $P < 0.05$), which were reversed by 7-HEC intervention ($P < 0.01$). This confirms that 7-HEC activates the PI3K/AKT signaling pathway, contributing to its protective effects in HAPE.

LY294002 Abolished the Protective Effects of 7-HEC Against HAPE

To elucidate the mechanism by which 7-HEC protects against HAPE via the PI3K/AKT signaling pathway, we examined the effect of LY294002-a specific PI3K/AKT inhibitor-in rats with HAPE. As shown in Figure 13A–C, the HAPE+LY group showed a decrease in the p-PI3K/PI3K and p-AKT/AKT ratios compared to the HAPE group, though the difference was not statistically significant. In contrast, 7-HEC treatment significantly increased both phosphorylation

https://doi.org/10.2147/DDDT.S541390

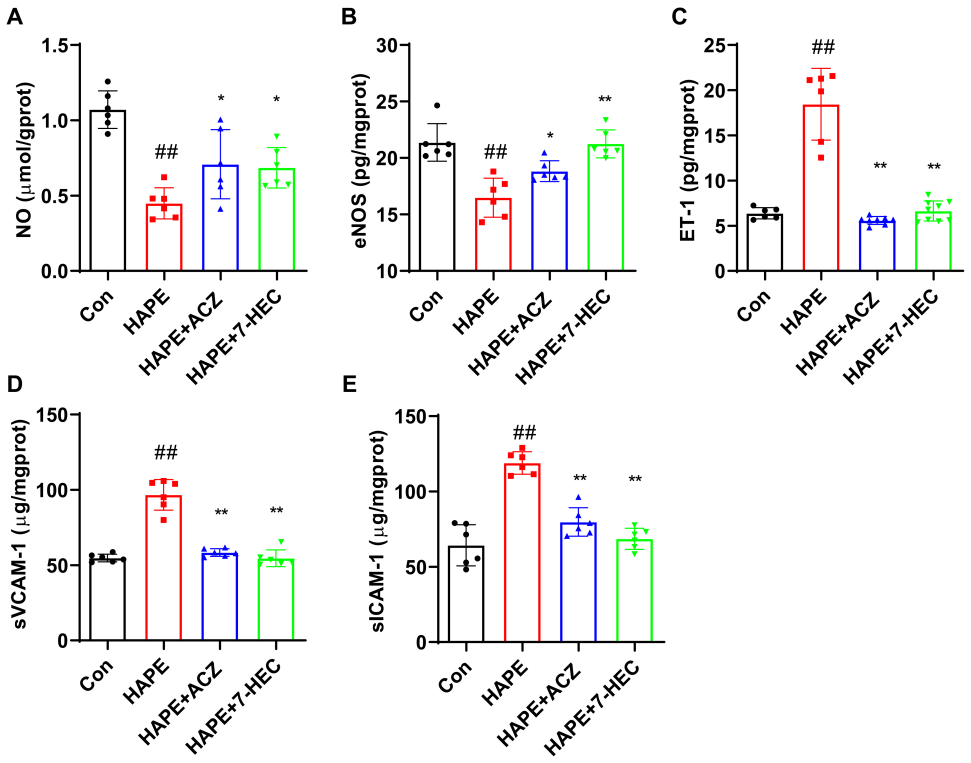

Figure 9 Effect of 7-HEC on endothelial function in the lung tissue of HAPE rats. (**A**) NO content, (**B**) eNOS content, (**C**) ET-1 content, (**D**) sVCAM-1 content, (**E**) sICAM-1 content. Data are presented as mean ± SD (n = 6). $^{\#\#}P < 0.01$ vs Con group; $^{*}P < 0.05$, $^{**}P < 0.01$ vs HAPE group.

ratios ($P < 0.01$), indicating activation of the PI3K/AKT pathway. However, this activation was almost completely suppressed by co-administration of LY294002.

Consistent with these molecular findings, Consistent with these molecular findings, LY294002 did not significantly affect lung water content (Figure 13D) or EB extravasation (Figure 13E), whereas 7-HEC significantly reduced both parameters ($P < 0.01$ for both). Notably, the reduction in LWC and EB content induced by 7-HEC was partially reversed by LY294002 co-treatment.

Histological evaluation via HE staining further supported these results. Both the HAPE and HAPE+LY groups exhibited similar pathological features of lung injury, including alveolar atrophy, thickening of alveolar walls, along with inflammatory cell infiltration and edema. In contrast, 7-HEC treatment markedly ameliorated these pathological changes (Figure 13F). However, co-treatment with LY294002 partially reversed this protective effect. Together, these results indicate that LY294002 abolishes the protective effects of 7-HEC against HAPE, underscoring the essential role of PI3K/AKT signaling in mediating the action of 7-HEC.

Discussion

HAPE receives growing concern due to the lack of effective drugs for its treatment or prevention. Novel drugs with high efficiency and low side effects are urgently needed. Our current study revealed that 7-HEC could alleviate HAPE by regulating oxidative stress and inflammation response via activation of the PI3K/AKT signaling pathway.

We first assessed the severity of HAPE by determining the LWC and found a notable increase in the LWC of HAPE rats compared to Con rats. We also observed a significant increase in pulmonary capillary permeability in HAPE rats by measuring the EB dye extravasation. HE staining further disclosed that the lung tissue of HAPE rats showed destroyed alveolar structure and thickened alveolar walls. However, treatment with 7-HEC reversed these changes, indicating that 7-HEC effectively mitigates HAPE.

HAPE is considered to be non-cardiogenic edema,[23] distinguished by the impaired alveolar barrier integrity and loss of alveolar fluid clearance.[24] To further evaluate the protective effect of 7-HEC against HAPE, we examined the

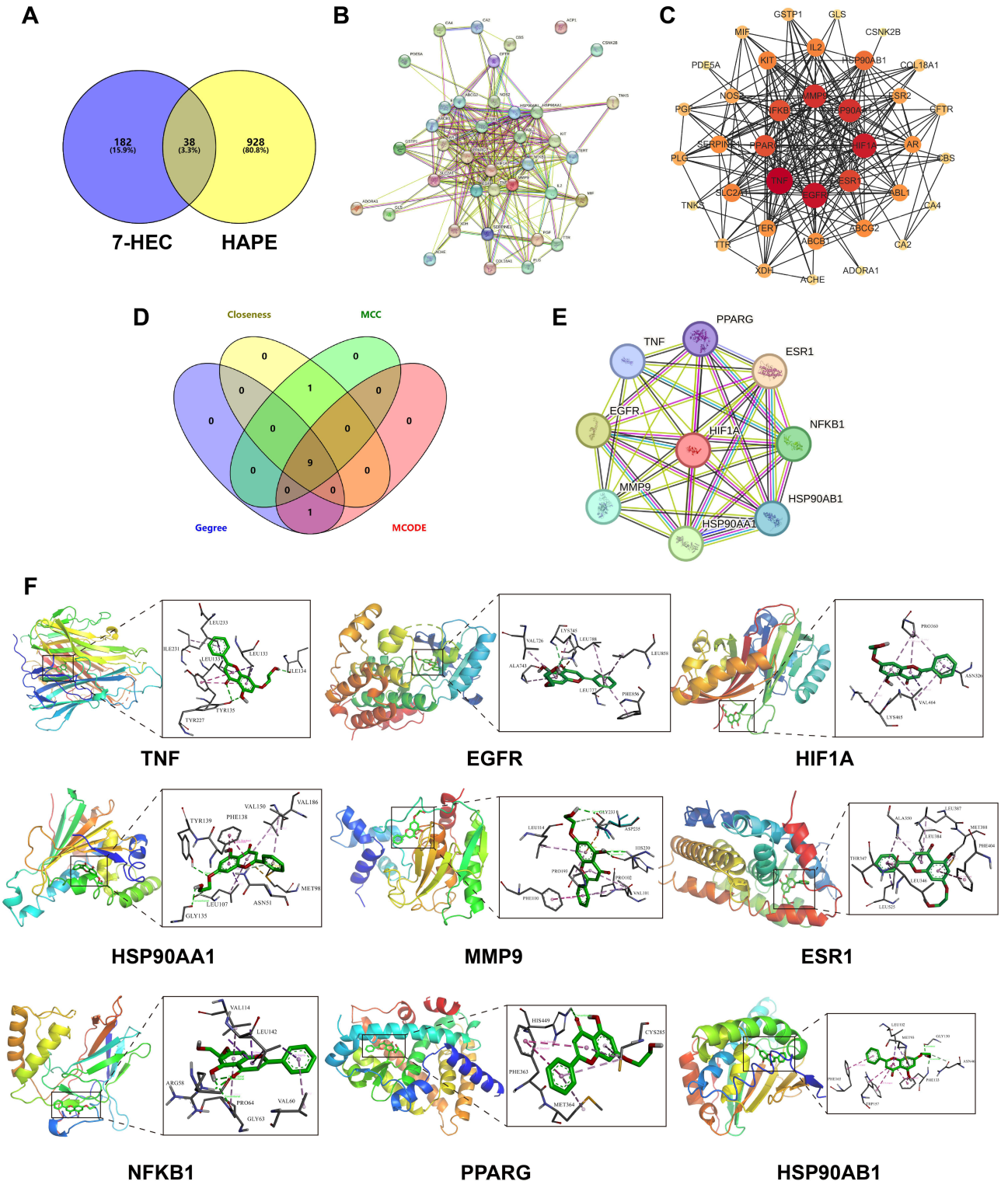

Figure 10 Hub targets analysis. (**A**) Venny diagram of 7-HEC target and HAPE target. (**B**) PPI network by STRING. (**C**) PPI network by Cytoscape. (**D**) Hub genes were identified using three algorithms of Cytohubba and MCODE. (**E**) 9 hub targets. (**F**) Visualization of the docking results between 7-HEC and hub targets.

expression of related genes and proteins in lung tissue. VEGF, a potent angiogenic factor, increases endothelial permeability and can cause pulmonary edema in mice.[25] HIF-1α is a hypoxia-induced transcription factor that regulates the subsequent expression of a variety of proteins, including VEGF.[26] Upregulation of HIF-1α has been reported to be associated with augmented pulmonary vascular barrier disruption.[27] One mechanism by which HH causes alveolar edema

https://doi.org/10.2147/DDDT.S541390

Table 3 Characteristics of the Hub Genes

Gene Name	Degree	Closeness Centrality	MCC	MCODE Score
TNF	29	32.5	6.06×10^{7}	9
EGFR	27	31.5	6.09×10^{7}	9
HIF1A	26	31	6.09×10^{7}	9
HSP90AA1	24	30	6.05×10^{7}	9
MMP9	24	30	5.57×10^{7}	9
ESR1	22	29	6.08×10^{7}	9
NFKB1	21	28.5	6.09×10^{7}	9
PPARG	21	28.5	5.49×10^{7}	9
HSP90AB1	18	27	6.02×10^{7}	9

Table 4 Molecular Docking Results

Gene Name	PDB or AlphaFold	Free Energy of Binding (kcal/mol)
TNF	7jra	−9.3
EGFR	8po4	−9.0
HIF1A	AF-Q16665-F1	−7.3
HSP90AA1	7s9h	−9.6
MMP9	8k5v	−8.7
ESR1	2qxs	−8.1
NFKB1	8tqd	−6.7
PPARG	3u9q	−9.0
HSP90AB1	6n8y	−9.1

is by increasing interstitial fluid accumulation through disruption of tight junctions.[28] Tight junction (TJ) proteins, including ZO-1, claudin, and occluding, are critical for maintaining the integrity of the lung epithelial barrier.[29] ENaC is an ion transporter that plays an important function in pulmonary edema by removing fluid from the alveolar space.[30] Dysfunction of ENaC, which inhibits alveolar fluid clearance, has also been implicated in the pathogenesis of HAPE.[31] AQP1, a selective water-channel protein, is abundantly expressed across the pulmonary microvascular endothelium and critically regulates fluid homeostasis. Previous studies have indicated that AQP1 protein levels are reduced in the lung tissue of HAPE rats, while Notoginsenoside R1 has been shown to increase AQP1 protein expression, thereby restoring its function in water molecule transport.[32] In this study, our results indicated that HH exposure up-regulated the mRNA expression of HIF-1α and VEGF and reduced the mRNA expression of Occludin, AQP1, and α-ENaC. In addition, we also found that HH led to an increase in the protein level of VEGF, while a decrease in the protein expression of Occludin and AQP1. These findings were in line with previous reports and indicated that alveolar barrier integrity and alveolar fluid clearance dysfunctions contributed to HAPE. Interestingly, 7-HEC pretreatment reversed the HH-induced changes, further proving that 7-HEC protects against HAPE.

Routine blood examination is a key part of the diagnosis and treatment of AMS. RBC and HGB, as key mediums for oxygen transport, were notably increased during HH.[33] Overproduction of these components can increase the cardiac load and cause brain-pulmonary circulation disorders. The changes in these indexes could be ameliorated by 7-HEC. In addition, the inflammatory response to HH results in elevated number of WBC, PLT, NEUT, and LYM compared to normal levels, which can be inhibited by 7-HEC. Blood gas composition analysis further validated the results of the hematological analysis. HH can lead to decreases in PaO_2 SaO_2, and $PaCO_2$, leading to tissue hypoxia.[33] In addition, HH can induce metabolic acidosis, characterized by decreased of pH and bicarbonate (HCO_3^-) levels along with excessive production of LA in the blood,[34] resulting in acid-base imbalance in the body. Moreover, electrolytes are an important buffer system for maintaining acid-base balance in the body, while high altitude-hypoxia leads to electrolyte metabolism

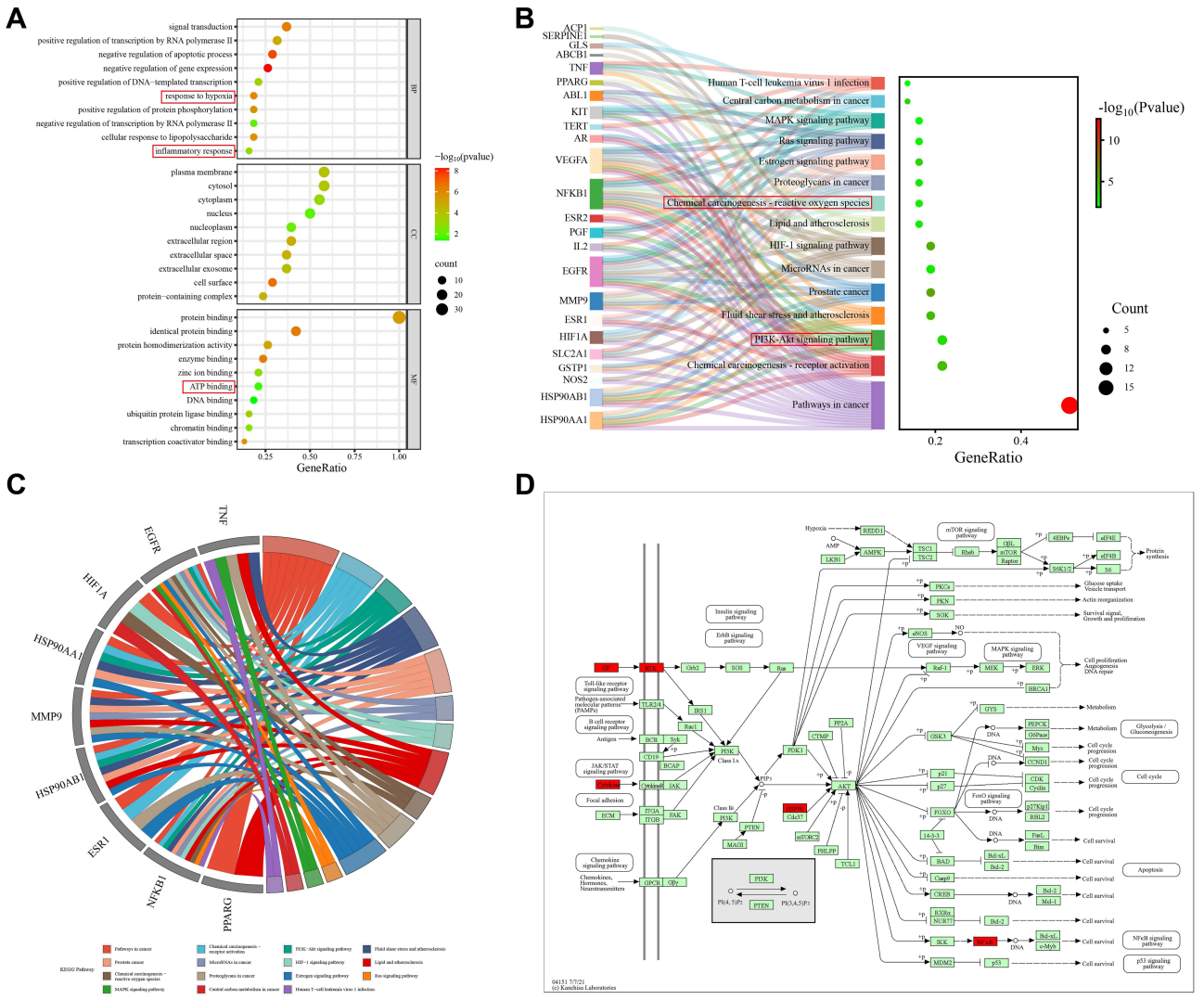

Figure 11 GO and KEGG enrichment analyses. (**A**) GO function enrichment analysis results. (**B**) KEGG pathway enrichment analysis results. The red boxes represent the important terms and pathways of 7-HEC against HAPE. (**C**) The top 15 pathways of hub genes. (**D**) Map of the PI3K/AKT signaling pathway. Targets marked in red represent potential targets of 7-HEC against HAPE.

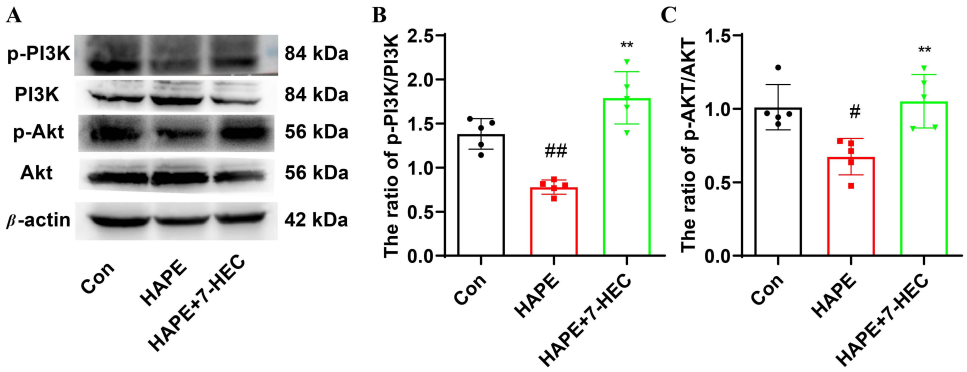

Figure 12 Effect of 7-HEC on the PI3K/AKT signaling pathway in the lung tissue of HAPE rats. (**A**) Relative protein expression of PI3K, p-PI3K, AKT, and p-AKT in lung tissue detected by Western blotting. Quantitative analysis of the ratios of p-PI3K/PI3K (**B**) and p-AKT/AKT (**C**). Data are presented as mean ± SD (n = 5). $^{\#}P < 0.05$, $^{\#\#}P < 0.01$ vs Con group; $^{**}P < 0.01$ vs HAPE group.

https://doi.org/10.2147/DDDT.S541390

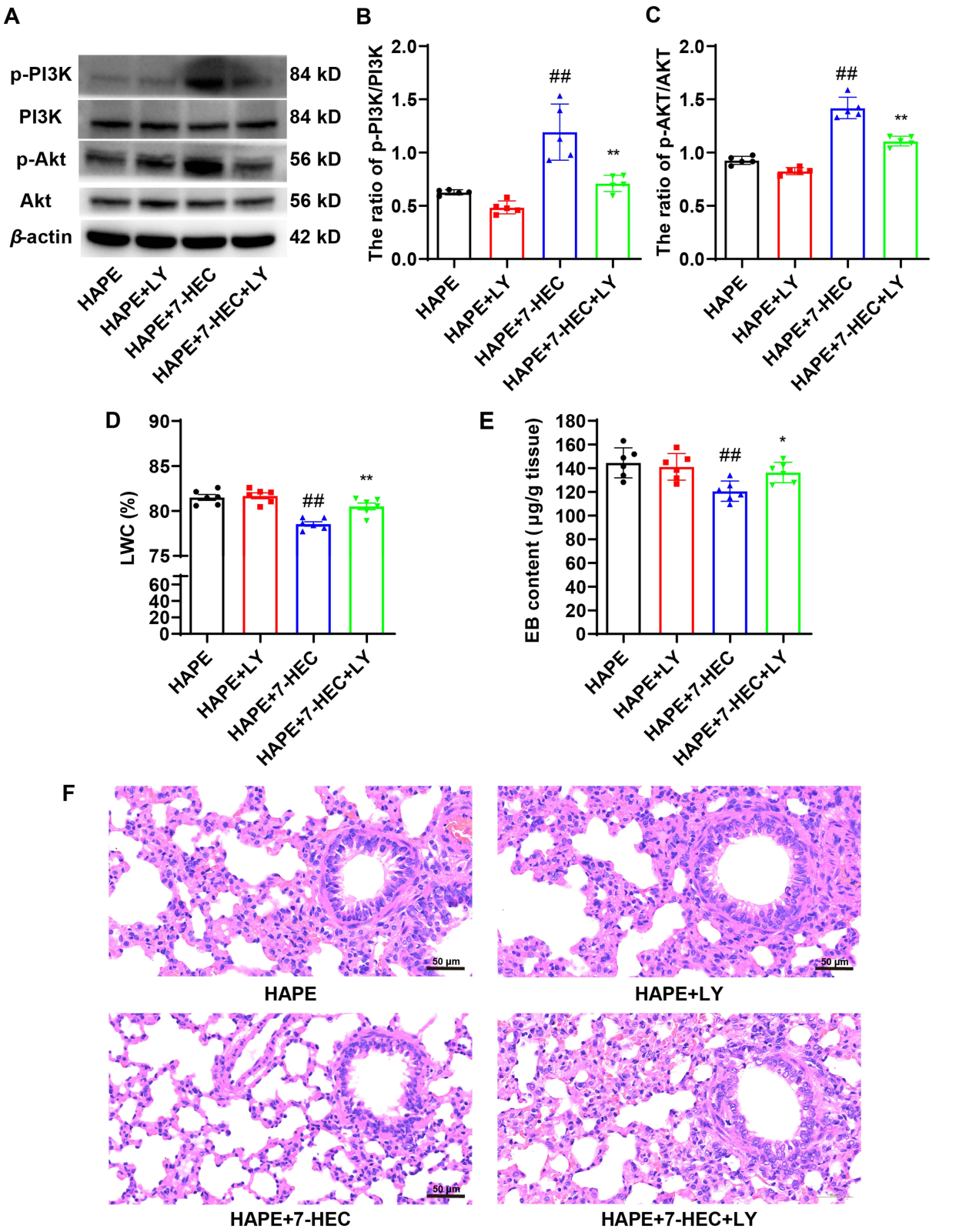

Figure 13 LY294002 abolished the protective effects of 7-HEC against HAPE. (**A**) Relative protein expression of PI3K, p-PI3K, AKT, and p-AKT in lung tissue detected by Western blotting. Quantitative analysis of the ratios of p-PI3K/PI3K (**B**) and p-AKT/AKT (**C**). (**D**) Lung water content. (**E**) EB leakage. Data are presented as mean ± SD (n = 5 or 6). $^{\#\#}P < 0.01$ vs HAPE group; $^{*}P < 0.05$, $^{**}P < 0.01$ vs 7-HEC group. (**F**) Histopathological changes of lung tissues observed by HE staining. Scale bar: 50 μm.

disorder.[35] These changes in HAPC rats were ameliorated following 7-HEC treatment, indicating its ability to counteract HAPE-induced arterial blood gas and routine blood abnormalities.

It is now widely accepted that one of main pathophysiology of HAPE is driven by an aggressive oxidative stress induced by HH.[12,36] HH exposure promotes the overproduction of ROS, leading to oxidative stress and lipid peroxidation.[37] MDA, a byproduct of lipid peroxidation, reflects the degree of oxidative damage. Excessive ROS can impair the structure and function of proteins and nucleic acids, leading to cell damage. Under HH conditions, increased production of free radicals is accompanied by the attenuation in intracellular antioxidant defense system. The primary antioxidant systems include enzymatic antioxidants (CAT, GSH-Px, SOD) and non-enzymatic antioxidants (GSH, vitamin C, vitamin E).[38] It is reported that increased oxidative stress in HAPE patients may be due to decreased SOD activity.[39] GST is a major Phase II detoxifying enzyme that protects living cells by catalyzing the binding of GSH to various endogenous and exogenous electrophilic molecules.[40] MPO is an indicator of oxidative stress injury and its activity is regarded as a particular indication of neutrophil infiltration and ALI severity.[41] MPO inhibition has been shown to reduce oxidative stress and preserve alveolar-capillary barrier function, representing a promising therapeutic strategy for HAPE.[42] In this research, we also observed increased levels of H_2O_2, MDA, and MPO, accompanied by decreased activities of SOD, CAT, GSH-Px, GST, and T-AOC, as well as reduced GSH content in HAPE rats. 7-HEC treatment effectively normalized these oxidative stress markers. These findings were consistent with the expected outcomes, suggesting that 7-HEC mitigates HAPE via inhibiting lipid peroxidation and oxidative stress.

HH caused oxidative stress is closely related to the inflammatory process.[43] Although some controversy remains,[44] accumulating evidence supports the critical role of inflammation in the pathogenesis of HAPE.[45,46] A study has reported that HH exposure leads to increased TNF-α, interleukins (IL-1, IL-2, IL-6), and C-reactive protein (CRP) in the blood.[47] These inflammatory factors further invade the lungs, inducing pneumonic inflammation that ultimately triggers HAPE.[48] NF-κB is a key proinflammatory signaling molecule that regulates the release of inflammatory cytokines in lung tissue under HH circumstances.[49] In this study, several proinflammatory cytokines, such as TNF-α, IL-1β, and IL-6, remarkably increased in the serum of rats with HAPE. 7-HEC treatment reduced the release of these cytokines in serum. In addition, we also found that the expressions of NF-κB p65 mRNA and p-NF-κB p65 protein were significantly increased in the lung tissue of HAPE rats, which was consistent with recent studies.[50,51] 7-HEC treatment reversed these changes. These findings suggest that 7-HEC alleviates inflammation response by suppressing of NF-κB activation and downstream cytokine production.

HH disrupts the energy supply, leading to severe energy metabolism disorders, which contribute to an abnormally high intracellular calcium ion concentration and trigger cellular damage. Molecular oxygen is required for mammalian cells to produce ATP as an energy source via oxidative phosphorylation (OXPHOS) in mitochondria. Under hypoxic environments, however, glycolysis becomes the main source of energy.[52] During glycolysis, PK catalyzes the irreversible conversion of ADP and phosphoenolpyruvate to ATP and PA.[53] PA is subsequently converted to LD by LDH.[54] Elevated LD level is an indicator of anaerobic glycolysis. ATP is hydrolyzed to ADP and phosphate ions by ATPase, and energy is released during hydrolysis process.[55] The important role of Na^+-K^+-ATPase in pulmonary edema clearance is well established.[31,56] Paul et al demonstrated that HH exposure induced lung injury is associated with energy metabolism disorders, as evidenced by the reduced ATP level and HDL/LDL ratio, as well as increased NAD/NADH ratio.[57] A recent study indicated that caffeine alleviated HAPE by controlling mitochondria quality and then maintaining ATP production.[58] In this study, we observed decreased ATP content and ATPase activity along with increased levels of LD, LDH, PK and PA in the lung tissue of HAPE rats. 7-HEC treatment reversed these changes, indicating that energy metabolism dysfunction in the lung tissue of HAPE rats was mitigated by 7-HEC.

Pulmonary vascular endothelial dysfunction contributes to the development of HAPE.[11] To assess endothelial function, we detected related factors including NO, eNOS, ET-1, sICAM-1, and sVCAM-1 in lung tissue. Previous study indicated that HH markedly impairs vascular endothelial function by decreasing bioavailability of NO. Impaired NO pathways may lead to enhanced hypoxic pulmonary vasoconstriction, which is a central pathogenesis of HAPE.[59] Reduced NOx levels and combination of heterozygotes are associated with the susceptibility to HAPE.[60] NO is produced by eNOS from L-Arg with O_2 and nicotinamide adenine dinucleotide phosphate (NADPH) as co-substrates.[61] ET-1, a robust vasoactive peptide released during injurious stimuli, is considered as a marker of endothelial dysfunction and

plays a pivotal role in pulmonary edema formation.[62] ICAM-1 and VCAM-1 belong to the immunoglobulin superfamily of cell adhesion molecules (CAM), and their overexpression is a hallmarks of endothelial dysfunction.[63] In this study, levels of NO and eNOS were greatly decreased, while the contents of ET-1, sICAM-1, and sVCAM-1 were significantly raised in the lung tissue of HAPE rats, indicating impaired endothelial function. 7-HEC treatment reversed these changes, suggesting that endothelial dysfunction in the lung tissue of HAPE rats was mitigated by 7-HEC.

To clarify the underlying mechanism of multi-target drug treatment of diseases at the molecular level, network pharmacology has been widely applied. In this study, we used a network pharmacology technique to extensively analyze the potential mechanisms of 7-HEC against HAPE. The results identified 38 potential therapeutic targets of 7-HEC against HAPE. PPI network analysis and molecular docking studies indicated that TNF, EGFR, HIF1A, HSP90AA1, MMP9, ESR1, NFKB1, PPARG, HSP90AB1 were the hub targets. Subsequently, GO and KEGG enrichment analyses demonstrated significant enrichment of the PI3K/AKT signaling pathway. Notably, four hub genes-NFKB1, EGFR, HSP90AB1, and HSP90AA1-were closely associated with this pathway. Among these, NFKB1 acts as a key downstream effector of PI3K/AKT and regulates inflammatory responses. EGFR can activate PI3K/AKT to promote cell survival and proliferation.[64] HSP90AB1 and HSP90AA1, as molecular chaperones, facilitate the stability and activation of multiple key components within the PI3K/AKT cascade.[65,66] These results indicate that 7-HEC may be effective in the treatment of HAPE by modulation of the oxidative stress and inflammatory response via PI3K/AKT signaling pathways.

The PI3K/AKT signaling pathway is an essential signal transduction mechanism that controls biological processes like cell survival, cell growth, and cell cycle progression.[67] PI3K upregulates downstream AKT expression by promoting the synthesis of phosphatidylinositol 3,4,5-trisphosphate (PIP3).[68] As the core of the pathway, AKT positively controls Nrf2 to enhance cellular resilience to oxidative stress and negatively regulates NF-κB to suppress the expression of pro-inflammatory factors.[69,70] Suppression of the PI3K/AKT signaling pathway has also been implicated in the pathophysiology of harm caused by HH, such as cerebral edema,[71] lung injury,[72] myocardial injury,[73] and pulmonary hypertension.[74] A recent study has indicated that ginsenoside Rg3 effectively alleviates HAPE by activating the PI3K/AKT signaling pathway and coordinately modulating inflammatory responses, oxidative stress, and ferroptosis.[75] In this study, we determined the effect of 7-HEC on the PI3K/AKT signaling pathway and observed that the ratios of p-PI3K/PI3K and p-AKT/AKT were decreased in the lung tissue of HAPE rats indicating the inhibition of PI3K/AKT signaling pathway. Treatment with 7-HEC reversed these changes, further verified the network pharmacology results. Furthermore, the protective effects of 7-HEC against HAPE were significantly attenuated by the selective PI3K/AKT inhibitor LY294002. These findings collectively indicate that 7-HEC activates the PI3K/AKT signaling pathway to exert protective effects against HAPE.

Nevertheless, this study has several limitations. First, the direct interaction between 7-HEC and the identified hub targets has not been experimentally validated, which should be addressed in future research. Second, further investigations will focus on interfering with the PI3K/AKT signaling pathway using specific inhibitors or lentiviral transduction techniques to substantiate our conclusions. Finally, while the current study examined the role of the PI3K/AKT signaling pathway in the protective effects of 7-HEC against HAPE, the involvement of other pathways such as MAPK signaling pathway and RAS signaling pathway remains unexplored and represents a promising direction for future mechanistic studies.

Conclusion

Taken together, our study reveals that pretreatment with 7-HEC reduces oxidative stress, inflammation response, energy metabolism disorder, and vascular endothelial dysfunction in rats suffering from HAPE. The beneficial effects of 7-HEC against HAPE are likely mediated through activation of the PI3K/AKT signaling pathway. These results suggest that 7-HEC is a promising therapeutic candidate for the prevention and treatment of HAPE.

Data Sharing Statement

The authors will provide the raw data without undue reservation to substantiate the conclusions of this article.

Ethics Statement

All animal experiments were approved by the Animal Care and Use Committee of 940th Hospital (No: 2015GKT017).

Author Contributions

All authors made a significant contribution to the work reported, whether that is in the conception, study design, execution, acquisition of data, analysis and interpretation, or in all these areas; took part in drafting, revising or critically reviewing the article; gave final approval of the version to be published; have agreed on the journal to which the article has been submitted; and agree to be accountable for all aspects of the work.

Funding

This work was funded by the National Natural Sciences Foundation of China (grant number 81202458) and Institutional Foundation of The First Affiliated Hospital of Xi'an Jiaotong University (grant number 2022MS-11).

Disclosure

The authors declare no competing financial interests or personal relationships that could have influenced the work presented in this paper.

References

1. Gatterer H, Villafuerte FC, Ulrich S, et al. Altitude illnesses. *Nat Rev Dis Primers*. 2024;10(1):43. doi:10.1038/s41572-024-00526-w
2. Korzeniewski K, Nitsch-Osuch A, Guzek A, Juszczak D. High altitude pulmonary edema in mountain climbers. *Respir Physiol Neurobiol*. 2015;209:33–38. doi:10.1016/j.resp.2014.09.023
3. Tian L, Zhao C, Yan Y, et al. Ceramide-1-phosphate alleviates high-altitude pulmonary edema by stabilizing circadian ARNTL-mediated mitochondrial dynamics. *J Adv Res*. 2024;60:75–92. doi:10.1016/j.jare.2023.07.008
4. Yang J, Jia Z, Song X, et al. Proteomic and clinical biomarkers for acute mountain sickness in a longitudinal cohort. *Commun Biol*. 2022;5(1):548. doi:10.1038/s42003-022-03514-6
5. Luks AM, Beidleman BA, Freer L, et al. Wilderness medical society clinical practice guidelines for the prevention, diagnosis, and treatment of acute altitude illness: 2024 update. *Wilderness Environ Med*. 2024;35(1_suppl):2s–19s. doi:10.1016/j.wem.2023.05.013
6. Luks AM, Hackett PH. Medical conditions and high-altitude travel. *N Engl J Med*. 2022;386(4):364–373. doi:10.1056/NEJMra2104829
7. Deshwal R, Iqbal M, Basnet S. Nifedipine for the treatment of high altitude pulmonary edema. *Wilderness Environ Med*. 2012;23(1):7–10. doi:10.1016/j.wem.2011.10.003
8. Luks AM, Auerbach PS, Freer L, et al. Wilderness medical society clinical practice guidelines for the prevention and treatment of acute altitude illness: 2019 update. *Wilderness Environ Med*. 2019;30(4s):S3–S18. doi:10.1016/j.wem.2019.04.006
9. Schmickl CN, Owens RL, Orr JE, Edwards BA, Malhotra A. Side effects of Acetazolamide: a systematic review and meta-analysis assessing overall risk and dose dependence. *BMJ Open Respir Res*. 2020;7(1):e000557. doi:10.1136/bmjresp-2020-000557
10. Burtscher M, Hefti U, Hefti JP. High-altitude illnesses: old stories and new insights into the pathophysiology, treatment and prevention. *Sports Med Health Sci*. 2021;3(2):59–69. doi:10.1016/j.smhs.2021.04.001
11. El Alam S, Pena E, Aguilera D, Siques P, Brito J. Inflammation in pulmonary hypertension and edema induced by hypobaric hypoxia exposure. *Int J Mol Sci*. 2022;23(20):12656. doi:10.3390/ijms232012656
12. Mao Z, Wang C, Liu J, et al. Superoxide dismutase 1-modified dental pulp stem cells alleviate high-altitude pulmonary edema by inhibiting oxidative stress through the Nrf2/HO-1 pathway. *Gene Ther*. 2024;31(7–8):422–433. doi:10.1038/s41434-024-00457-x
13. Jing L, Yang Y, Shao J, et al. Protective effect of 7-HEC on brain tissue damage induced by hypobaric hypoxia. *Chin J Mod Appl Pharm*. 2020;37(09):1025–1029. doi:10.13748/j.cnki.issn1007-7693.2020.09.001
14. Jing L, Yang Y, Shao J, et al. Protective effects and mechanism of 7-HEC against hypobaric hypoxia-induced cognitive impairments in rats. *Chin J Hosp Pharm*. 2020;40(15):1622–1626. doi:10.13286/j.1001-5213.2020.15.05
15. Zhang DM, Gao YH, Zhang J, Jing LL, Ma HP. Investigation on improvement effects and mechanism of 7-hydroxyethyl chrysin on PC12 cell injury induced by hypobaric hypoxia. *China Pharm*. 2023;34(04):402–406+412. doi:10.6039/j.issn.1001-0408.2023.04.04
16. Cai N, Liu TZ, Miao LW, et al. Protective effect and mechanism of 7-hydroxyethyl chrysin on hypoxia injury of cardiomyocytes. *Chin J Clin Pharmacol*. 2023;39(10):1417–1421. doi:10.13699/j.cnki.1001-6821.2023.10.011
17. Ma HP, Jing LL, Fang PC, et al. Synthesis of 7-hydroxyethyl chrysin and its application in the preparation of anti-hypoxic drugs. 9.
18. Tang D, Chen M, Huang X, et al. SRplot: a free online platform for data visualization and graphing. *PLoS One*. 2023;18(11):e0294236. doi:10.1371/journal.pone.0294236
19. Berger MM, Sareban M, Schiefer LM, et al. Effects of Acetazolamide on pulmonary artery pressure and prevention of high-altitude pulmonary edema after rapid active ascent to 4559 m. *J Appl Physiol*. 2022;132(6):1361–1369. doi:10.1152/japplphysiol.00806.2021
20. Zhang S, Wang N, Ma H, Jing L. A stable rat model of high altitude pulmonary edema established by hypobaric hypoxia combined diurnal temperature fluctuation and exercise. *Biochem Biophys Res Commun*. 2025;744:151193. doi:10.1016/j.bbrc.2024.151193
21. Jin Z, Li MY, Tang L, Zou Y, Chen K. Protective effect of Ulinastatin on acute lung injury in diabetic sepsis rats. *Int Immunopharmacol*. 2022;108:108908. doi:10.1016/j.intimp.2022.108908
22. Ogata H, Goto S, Sato K, et al. KEGG: kyoto encyclopedia of genes and genomes. *Nucleic Acids Res*. 1999;27(1):29–34. doi:10.1093/nar/27.1.29

23. Li Y, Zhang Y, Zhang Y. Research advances in pathogenesis and prophylactic measures of acute high altitude illness. *Respir Med*. 2018;145:145–152. doi:10.1016/j.rmed.2018.11.004
24. M T, T A, B S, Ak G, Sks S. Curcumin prophylaxis refurbishes alveolar epithelial barrier integrity and alveolar fluid clearance under hypoxia. *Respir Physiol Neurobiol*. 2020;274:103336. doi:10.1016/j.resp.2019.103336
25. Kaner RJ, Ladetto JV, Singh R, et al. Lung overexpression of the vascular endothelial growth factor gene induces pulmonary edema. *Am J Respir Cell Mol Biol*. 2000;22(6):657–664. doi:10.1165/ajrcmb.22.6.3779
26. Soree P, Gupta RK, Singh K, et al. Raised HIF1α during normoxia in high altitude pulmonary edema susceptible non-mountaineers. *Sci Rep*. 2016;6:26468. doi:10.1038/srep26468
27. Qi B, Chen HL, Shang D, et al. Effects of hypoxia-inducible factor-1α and matrix metalloproteinase-9 on alveolar-capillary barrier disruption and lung edema in rat models of severe acute pancreatitis-associated lung injury. *Exp Ther Med*. 2014;8(3):899–906. doi:10.3892/etm.2014.1810
28. Richalet JP, Jeny F, Callard P, Bernaudin JF. High-altitude pulmonary edema: the intercellular network hypothesis. *Am J Physiol Lung Cell Mol Physiol*. 2023;325(2):L155–L173. doi:10.1152/ajplung.00292.2022
29. Liu M, Gu C, Wang Y. Upregulation of the tight junction protein occludin: effects on ventilation-induced lung injury and mechanisms of action. *BMC Pulm Med*. 2014;14:94. doi:10.1186/1471-2466-14-94
30. Fei X, Ziqian Y, Bingwu Y, et al. Aldosterone alleviates lipopolysaccharide-induced acute lung injury by regulating epithelial sodium channel through PI3K/Akt/SGK1 signaling pathway. *Mol Cell Probes*. 2021;57:101709. doi:10.1016/j.mcp.2021.101709
31. Baloglu E, Nonnenmacher G, Seleninova A, et al. The role of hypoxia-induced modulation of alveolar epithelial Na(+)- transport in hypoxemia at high altitude. *Pulm Circ*. 2020;10(1 Suppl):50–58. doi:10.1177/2045894020936662
32. Pei C, Jia N, Wang Y, et al. Notoginsenoside R1 protects against hypobaric hypoxia-induced high-altitude pulmonary edema by inhibiting apoptosis via ERK1/2-P90rsk-BAD ignaling pathway. *Eur J Pharmacol*. 2023;959:176065. doi:10.1016/j.ejphar.2023.176065
33. Tripathi A, Hazari PP, Mishra AK, Kumar B, Sagi SSK. Quercetin: a savior of alveolar barrier integrity under hypoxic microenvironment. *Tissue Barriers*. 2021;9(2):1883963. doi:10.1080/21688370.2021.1883963
34. Liu F, Sui X, Wang Q, et al. Insights into the pharmacodynamics and pharmacokinetics of meldonium after exposure to acute high altitude. *Front Pharmacol*. 2023;14:1119046. doi:10.3389/fphar.2023.1119046
35. Murray AJ, Montgomery HE, Feelisch M, Grocott MPW, Martin DS. Metabolic adjustment to high-altitude hypoxia: from genetic signals to physiological implications. *Biochem Soc Trans*. 2018;46(3):599–607. doi:10.1042/BST20170502
36. Wang Y, Shen Z, Pei C, et al. Eleutheroside B ameliorated high altitude pulmonary edema by attenuating ferroptosis and necroptosis through Nrf2-antioxidant response signaling. *Biomed Pharmacother*. 2022;156:113982. doi:10.1016/j.biopha.2022.113982
37. Pena E, El Alam S, Siques P, Brito J. Oxidative stress and diseases associated with high-altitude exposure. *Antioxidants*. 2022;11(2):267. doi:10.3390/antiox11020267
38. Jena AB, Samal RR, Bhol NK, Duttaroy AK. Cellular Red-Ox system in health and disease: the latest update. *Biomed Pharmacother*. 2023;162:114606. doi:10.1016/j.biopha.2023.114606
39. Sharma S, Singh Y, Sandhir R, et al. Mitochondrial DNA mutations contribute to high altitude pulmonary edema via increased oxidative stress and metabolic reprogramming during hypobaric hypoxia. *Biochim Biophys Acta Bioenergy*. 2021;1862(8):148431. doi:10.1016/j.bbabio.2021.148431
40. Mazari AMA, Zhang L, Ye ZW, et al. The multifaceted role of glutathione s-transferases in health and disease. *Biomolecules*. 2023;13(4):688. doi:10.3390/biom13040688
41. Zeng Y, Cao W, Huang Y, et al. Huangqi Baihe Granules alleviate hypobaric hypoxia-induced acute lung injury in rats by suppressing oxidative stress and the TLR4/NF-κB/NLRP3 inflammatory pathway. *J Ethnopharmacol*. 2024;324:117765. doi:10.1016/j.jep.2024.117765
42. Zhang H, Wang X, Liu J, et al. Role of neutrophil myeloperoxidase in the development and progression of high-altitude pulmonary edema. *Biochem Biophys Res Commun*. 2024;703:149681. doi:10.1016/j.bbrc.2024.149681
43. Pena E, Brito J, El Alam S, Siques P. Oxidative stress, kinase activity and inflammatory implications in right ventricular hypertrophy and heart failure under hypobaric hypoxia. *Int J Mol Sci*. 2020;21(17):6421. doi:10.3390/ijms21176421
44. Swenson ER, Maggiorini M, Mongovin S, et al. Pathogenesis of high-altitude pulmonary edema: inflammation is not an etiologic factor. *JAMA*. 2002;287(17):2228–2235. doi:10.1001/jama.287.17.2228
45. Nussbaumer-Ochsner Y, Schuepfer N, Ursprung J, et al. Sleep and breathing in high altitude pulmonary edema susceptible subjects at 4559 meters. *Sleep*. 2012;35(10):1413–1421. doi:10.5665/sleep.2126
46. Sharma M, Singh SB, Sarkar S. Genome wide expression analysis suggests perturbation of vascular homeostasis during high altitude pulmonary edema. *PLoS One*. 2014;9(1):e85902. doi:10.1371/journal.pone.0085902
47. Hilty MP, Zügel S, Schoeb M, et al. Soluble urokinase-type plasminogen activator receptor plasma concentration may predict susceptibility to high altitude pulmonary edema. *Mediators Inflamm*. 2016;2016:1942460. doi:10.1155/2016/1942460
48. Bailey DM, Kleger GR, Holzgraefe M, Ballmer PE, Bärtsch P. Pathophysiological significance of peroxidative stress, neuronal damage, and membrane permeability in acute mountain sickness. *J Appl Physiol*. 2004;96(4):1459–1463. doi:10.1152/japplphysiol.00704.2003
49. Sarada S, Himadri P, Mishra C, et al. Role of oxidative stress and NFkB in hypoxia-induced pulmonary edema. *Exp Biol Med*. 2008;233(9):1088–1098. doi:10.3181/0712-rm-337
50. Yang X, Dong X, Li J, et al. Nanocurcumin attenuates pyroptosis and inflammation through inhibiting NF-κB/GSDMD signal in high altitude-associated acute liver injury. *J Biochem Mol Toxicol*. 2024;38(1):e23606. doi:10.1002/jbt.23606
51. Pham K, Parikh K, Heinrich EC. Hypoxia and inflammation: insights from high-altitude physiology. *Front Physiol*. 2021;12:676782. doi:10.3389/fphys.2021.676782
52. Wang D, Liu F, Yang W, et al. Meldonium ameliorates hypoxia-induced lung injury and oxidative stress by regulating platelet-type phosphofructokinase-mediated glycolysis. *Front Pharmacol*. 2022;13:863451. doi:10.3389/fphar.2022.863451
53. Schormann N, Hayden KL, Lee P, Banerjee S, Chattopadhyay D. An overview of structure, function, and regulation of pyruvate kinases. *Protein Sci*. 2019;28(10):1771–1784. doi:10.1002/pro.3691
54. Shibata S, Sogabe S, Miwa M, et al. Identification of the first highly selective inhibitor of human lactate dehydrogenase B. *Sci Rep*. 2021;11(1):21353. doi:10.1038/s41598-021-00820-7
55. Zhao T, Tan L, Han X, et al. Energy metabolism response induced by microplastic for marine dinoflagellate Karenia mikimotoi. *Sci Total Environ*. 2023;866:161267. doi:10.1016/j.scitotenv.2022.161267

56. Nehra S, Bhardwaj V, Bansal A, Saraswat D. Nanocurcumin accords protection against acute hypobaric hypoxia induced lung injury in rats. *J Physiol Biochem*. 2016;72(4):763–779. doi:10.1007/s13105-016-0515-3
57. Paul S, Gangwar A, Bhargava K, Ahmad Y. D4F prophylaxis enables redox and energy homeostasis while preventing inflammation during hypoxia exposure. *Biomed Pharmacother*. 2021;133:111083. doi:10.1016/j.biopha.2020.111083
58. Tian L, Jia Z, Yan Y, et al. Low-dose of caffeine alleviates high altitude pulmonary edema via regulating mitochondrial quality control process in AT1 cells. *Front Pharmacol*. 2023;14:1155414. doi:10.3389/fphar.2023.1155414
59. Berger MM, Hesse C, Dehnert C, et al. Hypoxia impairs systemic endothelial function in individuals prone to high-altitude pulmonary edema. *Am J Respir Crit Care Med*. 2005;172(6):763–767. doi:10.1164/rccm.200504-654OC
60. Ahsan A, Mohd G, Norboo T, Baig MA, Pasha MA. Heterozygotes of NOS3 polymorphisms contribute to reduced nitrogen oxides in high-altitude pulmonary edema. *Chest*. 2006;130(5):1511–1519. doi:10.1378/chest.130.5.1511
61. Janaszak-Jasiecka A, Płoska A, Wierońska JM, Dobrucki LW, Kalinowski L. Endothelial dysfunction due to eNOS uncoupling: molecular mechanisms as potential therapeutic targets. *Cell Mol Biol Lett*. 2023;28(1):21. doi:10.1186/s11658-023-00423-2
62. Berger MM, Rozendal CS, Schieber C, et al. The effect of endothelin-1 on alveolar fluid clearance and pulmonary edema formation in the rat. *Anesth Analg*. 2009;108(1):225–231. doi:10.1213/ane.0b013e31818881a8
63. Habas K, Shang L. Alterations in intercellular adhesion molecule 1 (ICAM-1) and vascular cell adhesion molecule 1 (VCAM-1) in human endothelial cells. *Tissue Cell*. 2018;54:139–143. doi:10.1016/j.tice.2018.09.002
64. An SJ, Anneken A, Xi Z, et al. Regulation of EGF-stimulated activation of the PI-3K/AKT pathway by exocyst-mediated exocytosis. *Proc Natl Acad Sci U S A*. 2022;119(48):e2208947119. doi:10.1073/pnas.2208947119
65. Wang H, Deng G, Ai M, et al. Hsp90ab1 stabilizes LRP5 to promote epithelial-mesenchymal transition via activating of AKT and Wnt/β-catenin signaling pathways in gastric cancer progression. *Oncogene*. 2019;38(9):1489–1507. doi:10.1038/s41388-018-0532-5
66. Sato S, Fujita N, Tsuruo T. Modulation of Akt kinase activity by binding to Hsp90. *Proc Natl Acad Sci U S A*. 2000;97(20):10832–10837. doi:10.1073/pnas.170276797
67. Glaviano A, Foo ASC, Lam HY, et al. PI3K/AKT/mTOR signaling transduction pathway and targeted therapies in cancer. *Mol Cancer*. 2023;22 (1):138. doi:10.1186/s12943-023-01827-6
68. Kearney AL, Norris DM, Ghomlaghi M, et al. Akt phosphorylates insulin receptor substrate to limit PI3K-mediated PIP3 synthesis. *Elife*. 2021:10. doi: 10.7554/eLife.66942
69. Bayo Jimenez MT, Frenis K, Hahad O, et al. Protective actions of nuclear factor erythroid 2-related factor 2 (NRF2) and downstream pathways against environmental stressors. *Free Radic Biol Med*. 2022;187:72–91. doi:10.1016/j.freeradbiomed.2022.05.016
70. Fu C, Wu Y, Liu S, et al. Rehmannioside A improves cognitive impairment and alleviates ferroptosis via activating PI3K/AKT/Nrf2 and SLC7A11/GPX4 signaling pathway after ischemia. *J Ethnopharmacol*. 2022;289:115021. doi:10.1016/j.jep.2022.115021
71. Gong G, Yin L, Yuan L, et al. Ganglioside GM1 protects against high altitude cerebral edema in rats by suppressing the oxidative stress and inflammatory response via the PI3K/AKT-Nrf2 pathway. *Mol Immunol*. 2018;95:91–98. doi:10.1016/j.molimm.2018.02.001
72. Li N, Cheng Y, Jin T, et al. Kaempferol and ginsenoside Rg1 ameliorate acute hypobaric hypoxia induced lung injury based on network pharmacology analysis. *Toxicol Appl Pharmacol*. 2023;480:116742. doi:10.1016/j.taap.2023.116742
73. Wang N, Song J, Zhou G, Li W, Ma H. Mechanism of salidroside relieving the acute hypoxia-induced myocardial injury through the PI3K/Akt pathway. *Saudi J Biol Sci*. 2020;27(6):1533–1537. doi:10.1016/j.sjbs.2020.04.035
74. Ji L, Su S, Xin M, et al. Luteolin ameliorates hypoxia-induced pulmonary hypertension via regulating HIF-2α-Arg-NO axis and PI3K-AKT-eNOS-NO signaling pathway. *Phytomedicine*. 2022;104:154329. doi:10.1016/j.phymed.2022.154329
75. He Y, Wang Y, Duan H, et al. Pharmacological targeting of ferroptosis in hypoxia-induced pulmonary edema: therapeutic potential of ginsenoside Rg3 through activation of the PI3K/AKT pathway. *Front Pharmacol*. 2025;16:1644436. doi:10.3389/fphar.2025.1644436